RADIATION LEVELS IN SELECTED CERAMIC BUILDING TILE BRANDS USED IN KENYA

JAMES NGUNDI KITHEKA

A Thesis Submitted in Partial Fulfillment of the Requirements for the Degree of Master of Science in Physics of South Eastern Kenya University

2023

DECLARATION

This presentation is my own original work which has not been used earlier anywhere for the award of any certificate.

Signature..... Date.....

James Ngundi Kitheka

I423/KIT/20050/2017

This thesis has been submitted for examination with our approval as University Supervisors.

Signature..... Date.....

Dr. Mugambi J. Linturi

Department of Physical Sciences.

South Eastern Kenya University.

Signature..... Date.....

Dr. Onesmus Maweu

Department of Physical Sciences.

South Eastern Kenya University.

ACKNOWLEDGEMENT

Firstly, I thank the lord God almighty for the good health he has accorded me and the reasoning to begin this course. He has given me the capacity to think soberly and overcome any hurdles in the way of this work.

I register sincere gratitude to my able and committed supervisors Dr. Mugambi Linturi and Dr Onesmus Maweu for their consistent advice and encouragement all the way from selecting a research topic, proposal development and presentation. Their wide experience in radiation detection and measurement, data collection and analysis were paramount in building this thesis. I cannot forget to salute all my South Eastern Kenya University physics lecturers for their teaching support from class work to even beginning the proposal writing. God bless them.

I sincerely thank my dear wife Catherine Mutindi, my children Joshua Kitheka, Jolly Keziah and Jomie Riches. They have always supported me and given me a conducive environment to do my work and encouraged me not to tire up.

My parents Jackson Kitheka and Lydia Muthina told me that, for one to remain relevant, he/she must climb the ladder of academics. This gave me enough courage to go on with the work.

The determination of my workmates in academic advancement at ABC KISOVO SEC SCHOOL has always given me a moral drive ferrying me strong in the ups and downs of this study.

Lastly, I wish to register sincere gratitude to the ministry of mining and petroleum Nairobi-Kenya headquarters for giving me time and grace to use their laboratory for measurements and crushing of my tile samples to powder.

DEDICATION

I dedicate my thesis to my dear wife Catherine Mutindi, family, siblings and to all my friends for their undivided financial, moral and spiritual assistance which energized me enough to conduct this research.

TABLE OF CONTENTS

CHAPTER FOUR

LIST OF TABLES

LIST OF FIGURES

LIST OF APPENDICES

ABBREVIATIONS AND ACRONYMS

KRPB	**:**	Kenya Radiation Protection Board
UNSCEAR	**:**	United Nations Scientific Committee on Effects of Atomic Radiations
NRPB	**:**	National Radiation Protection Board
NORE	**:**	Naturally Occurring Radioactive Elements
CCR	**:**	Consumer Confidence Report
IAEA	**:**	International Atomic Energy Association
HIBRA	**:**	High Background Radiation Area
ICRP	**:**	International Commission for Radiation Protection
KNBS	**:**	Kenya National Bureau of Statistics
ADC	**:**	Analogue to Digital Converter
LAN	**:**	Local Area Network
FWHM	**:**	Full Width at Half Maximum
MCA	**:**	Multi Channel Analyzer
MCB	**:**	Multi Channel buffer
SEKU	**:**	South Eastern Kenya University
KNRA	**:**	Kenya Nuclear Regulatory Authority
WHO	**:**	World Health Organization
USD	**:**	United States Dollar
DNA	**:**	Deoxyribonucleic Acid
WIFI	**:**	Wireless Fidelity
USB	**:**	Universal Serial Bus
AED	**:**	Annual Effective Dose
LET	**:**	Linear Energy Transfer
NRA	**:**	National Regulatory Authority
RNA	**:**	Ribonucleic Acid
KE	**:**	Kinetic Energy
KERMA	**:**	Kinetic Energy Released Per unit Mass

ABSTRACT

Radiations of both natural and artificial origin are readily available in the environment. Building materials like stones, cement, ceramics, water and sand contain radioactive nuclides, which are harmful to mankind. Elevated levels of radiation from these materials are potential causes of prompt or delayed harmful effects to human health. The ceramic tiles which were the focus of this study are made from mixture of earthly matter including kaolin, quarts, talc and feldspar which contain primordial radioisotopes like Thorium-232(^{232}Th), Potassium-40(^{40}K) and Uranium-238(^{238}U) known to release radiations. This study was aimed at establishing the levels of radiations from ceramic building tiles used in Kenya. A total of 37 samples of tiles from different countries and manufacturers were analyzed. Thallium doped sodium iodide gamma-ray counter (NaI (TI)) was used for data acquisition. A mean activity concentration of 53.73±2.34BqKg^{-1} for ^{232}Th, 43.17±3.40BqKg^{-1} for ^{238}U and 525.99±36.10BqKg^{-1} for ^{40}K was obtained. The comparison of the obtained activity concentration values with other related studies indicated that the activity of the radio nuclides is dependent on the geological composition of the raw material source. Using the activity concentration values obtained, the dose rates and the hazard indices thereof were calculated. Mean values for radium equivalent activity, absorbed dose, indoor and outdoor annual effective dose, and hazard indices (internal and external) obtained were 159.59BqKg^{-1}, 75.55nGyh^{-1}, 0.28, 0.19, 0.54 and 0.43 respectively. The highest recorded value of hazard index (both internal and external) was found to be 0.92 while the lowest was 0.15 which are both below the world's safety limit of a unit recommended in the International Commission for Radiation Protection (ICRP) reports. Generally, the ceramic building tiles in the Kenyan market as at the time of this study were safe for human handling as seen from the radiological parameters.

CHAPTER ONE

1.0 INTRODUCTION

1.1 Study Background

Radioactivity refers to the emission and transmission of particles/radiations by disintegrating atomic nuclei. This radiation deposits energy in matter as it gets attenuated in its flight path. The earth and the life in it have been constantly exposed to such radiation of artificial and natural origin. Artificial radiation originates from medical diagnostics, treatments during medical procedure and dosage as well as application of phosphate fertilizers to soils in agriculture. Natural radioactivity includes cosmic rays from the outer space and terrestrial radiation. The intensity of cosmic radiation is dependent on altitude, thus people living in lowlands have minimal health effects due cosmic radiation exposure. The intensity of terrestrial radiation on the other hand depends on the geographical and geological formations of an area and is present in all regions of the earth (UNSCEAR, 2000). Radiation levels of a given soil is related to the rock type from which the soil is obtained with igneous rocks like granites being associated with higher values of radiation and sedimentary rocks lower radiations(UNSCEAR, 2000).

Radiations of different magnitudes are encountered in every day-to-day life. These radiations depending on the application intensity and time of exposure are both beneficial if used in the right way and harmful in case of long exposure or excessive dosage(UNSCEAR, 2000). They are broadly categorized as non-ionizing and ionizing radiation. Non-ionizing radiation which includes microwaves, radio waves, visible light among others, do not have enough energy to ionize matter and is harmless unless at very high doses. Ionizing radiation which was the interest in this work include among others, x-rays and gamma rays which can strike electrons off atomic orbitals hence ionizing the particles they pass through. Figure1.1 shows various sources of radiation in percentage.

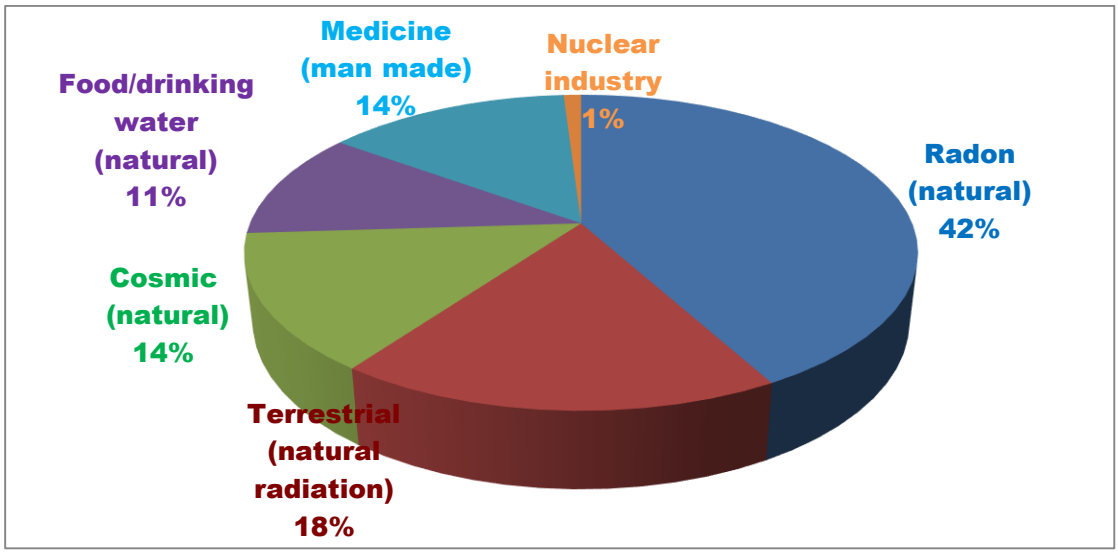

Figure1.1: Annual Percentage of the Radiation Dose from Natural and Artificial Sources (UNSCEAR, 2000)

From figure 1.1, it is evident that natural radiation contributes the greatest percentage of the total radiation exposure. Terrestrial contributes the largest percentage (71%) of natural radiation exposure to humans. Ceramic building tiles which were the focus of this study fall in this category because their raw materials are earthly based. These raw materials include quartz (SiO_2), feldspar ($KAlSi_3O_8$), plastic clay ($Al_2O_{32}SiO_22H_2O$), kaolin ($Al_2Si_20_5$) and steatite (talc) ($Mg_3Si_4O_{10}(OH)_2$) which are all earthly matter generally known as mud (Richards, 1999).

All the raw materials listed are compounds of silicon, which is isotopic with Si-31 being radioactive. Aluminum-26 is a radioactive isotope with half-life of $7.2x10^5$ years while Magnesium which has 19 radioisotopes, ranging from Mg-18 to Mg-41, has its longest-lived radioisotope as Mg-28 with half-life of 20.915 hours. Tritium or hydrogen-3 is radioactive with half-life of 12.32 years while Potassium-40 with half-life of $1.28x10^9$ years is a well-known radioactive element. There is therefore a high possibility of radiations from ceramic building tiles(Dondi, 1999).

During the manufacture of tiles, mass proportioning of the raw materials is done before crushing them fine. Any waste is removed at the atomization stage and recycled. In the

case of dry milling, water is then added to produce a viscous paste of the clay. The paste is then molded to a tile shape, and then pressed at elevated temperatures, about 1093^0C to produce the tile. Finger 1.2 shows the stepwise production process.

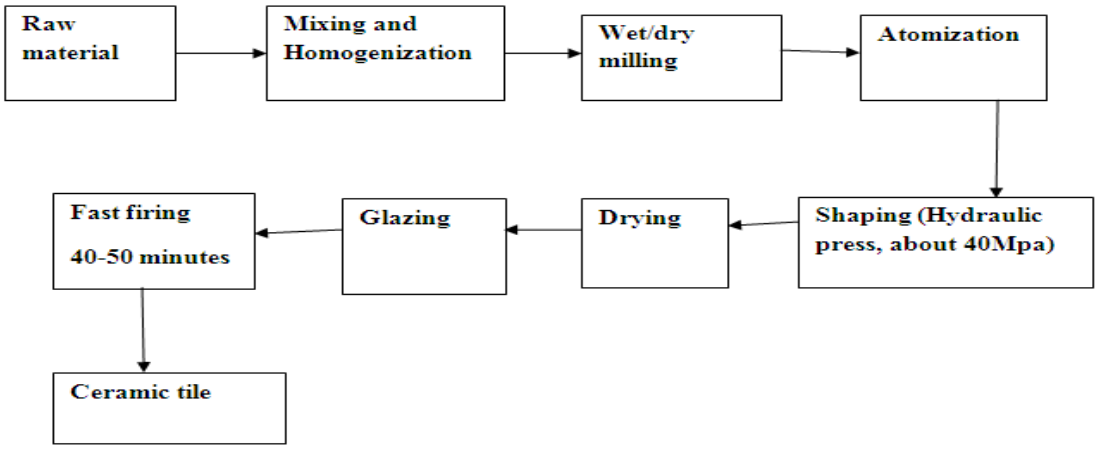

Figure 1.2: Ceramic Tile Production Process

Glazing (coat it with a liquid-colored glass called frit) is then done which incorporates zircon in the tile. The zircon makes the tile have higher natural radioactivity than that mean values for the materials used for building (Righi & Bruzzi, 2006). Most building materials contain radioisotopes like ^{226}Ra, ^{232}Th and ^{40}K which occur naturally (Khan*et al.*, 1998). These building materials are a source of gamma-ray exposure to human beings indoors (Ravisankar *et al.*, 2012);(Senthilkumar *et al.*, 2014); (Senthilkumar & Narayanaswamy, 2016) due to their natural radioisotope concentrations.

Ceramic tiles have proven to be durable and very attractive hence their mass inflow into the building market. This exposes human beings engaged with them to possible radiations from the tiles. External exposure may be due to gamma rays from ^{238}U, ^{232}Th and their progeny as well as ^{40}K. In the ^{238}U decay chain, Radium-226 (^{226}Ra) and its progenies contribute 98.5% of the total radiological effects of ^{238}U(Otwoma *et al.*, 2013), their precursors in the series do not release highly penetrating radiation and are therefore not radio logically significant. Internal exposure may be due to the radiation from radon whose

half-life is 3.8 days and its decay products when inhaled (Khan *et al.,* 1998);(Stoulos *et al.*, 2003).

The radio nuclides^{232}Th,^{238}U and ^{40}K originate from the earth's crust(Engelkemeir *et l.*, 1962); (Gaffney & Marley, 2006).

The radio nuclides break down spontaneously (natural radioactivity) releasing ionizing radiations with sufficient energy to destroy human body cells(Ferrari & Szuszkiewicz, 2022). The radiation effect a living body may get depends on the type, period of exposure, intensity of the radiation and also the type of organ exposed(`World Health Organization, 2016). If for example the energy of a gamma ray lies between 3MeV- 10MeV, then its harmful health effects may manifest immediately or after some time. Exposure to radiation exceeding the threshold set by bodies like world health organization, United Nations scientific committee on the effects of atomic radiation (UNSCEAR) and environmental protection agency (EPA) may result in complications like cancer, genetic mutation, and cataracts among others. Table 1.1presents the recommended thresholds for various radiological parameters by different organizations.

Table 1.1 Radiological Parameters and the Corresponding World's Recommended Thresholds

Parameter	Recommended limit	SI unit.	Recommending body
Absorbed dose	60nGyh^{-1}	Gyh^{-1}	(UNSCEAR, 2010)
Radium equivalent	370	BqKg^{-1}	(UNSCEAR, 1988)
Annual effective dose	1	Svy^{-1}	(ICRP, 2007)
External hazard index	1	_	(ICRP, 1993)
Internal hazard index	1	_	(ICRP, 1993)

The nuclides (^{238}U), (^{232}Th) and (^{40}K), are examples of radioactive isotopes that exist at detectable concentrations in earthly matter. Such radio nuclides move upwards from deep

down the earth as elements in underground water and by processes like mining and vulcanization. Their exposure on the surface of the earth makes our environment naturally radioactive and they may be harmful depending on their concentrations.

According to Mustapha (1999), Human beings in tropical countries like Kenya spend approximately 60% of their time indoors and therefore likely to be exposed to possible radiation from the building materials of which tiles is one. This study was aimed at determining the radiation levels of ceramic building tiles and establishing their health hazards to the house dwellers. This was done by determining the activity concentrations of radio nuclides uranium (^{238}U), thorium (^{232}Th) and potassium (^{40}K) in the tiles using gamma ray spectroscopy. The activity concentration in $BqKg^{-1}$ of the three radio nuclides was then used to determine the radiological parameters like radium equivalent, annual effective dose, internal and external hazard indices among others. The data obtained is important in providing vital information to radiation protection bodies like Kenya Nuclear Regulatory Authority (KNRA), International Commission on Radiological Protection (ICRP), policy makers and other researchers working on radiation related areas.

1.2 Statement of the Problem

In modern building and construction in Kenya and the World, ceramic tiles are being widely used as decorative building materials for walls and floors. The tiles are preferred for their appealing appearance, durability and the smooth moisture proof surface they provide. Since the raw materials of the tiles are mined from the earth's crust, they contain primordial radio nuclides like ^{232}Th, ^{238}U and ^{40}K. These radio nuclides and their progeny release radiations which are generally harmful to human beings depending on their concentrations. Studies show that human beings spend 60-80% of their time indoors. There is therefore a likelihood of human exposure to probable radiation from ceramic tiles used in the buildings. Transportation, loading and unloading the tiles in vehicles and storage also engage humans. Therefore, it was of great importance to study and establish the radiation levels of these tiles.

1.3 Objectives

1.3.1 General Objective

To determine the levels of natural radioactivity in selected ceramic building tiles commercially available in Kenya.

1.3.2 Specific Objectives

i. To determine the activity concentration, of ^{232}Th, ^{238}U and ^{40}K present in building tiles used in Kenya.
ii. To establish values of the radiological parameters (dose rates) of ^{232}Th, ^{238}U and ^{40}K in ceramic building tiles used in Kenya.

1.4 Research Questions

i. What is the activity concentration of ^{232}Th, ^{238}U and ^{40}K present in the ceramic tiles used in Kenya?
ii. What are the radiological parameters of; ^{232}Th, ^{238}U and ^{40}K in ceramic building tiles used in Kenya?

1.5 Justification of the Study

Natural radioactivity contributes up to 85% of human exposure to radiation. Since this radiation originates from the earth's crust, and the earth is a source of many building materials, it becomes a potential source of health problems to human beings using them. Ceramic tiles, whose origin is earthly matter, are used for interior decorations majorly for floors and walls. They are relatively cheap and thus accessible to a large population.

In Kenya the construction industry is thriving, and this prompts a large population to engage with the tiles. People may get exposure to radiation from the tiles during transportation, loading and offloading them in vehicles, storage of the tiles, using the tiles when building and living in the ceramic tiles finished houses. This means that a large population in Kenya interacts with these radiations at many given ways and times in their lives. If the natural radioactivity in the ceramic tiles exceeds the permissible thresholds, they pose a risk of harmful human exposure.

A few studies on radiation levels of ceramic tiles have been done in Kenya so far. It is therefore imperative to conduct more research in this field and enrich the radiation data bank in the country. Data obtained from this study provides information to regulatory bodies like World Health Organization (WHO), Kenya Nuclear Regulatory Authority (KNRA) and National Radiation Protection Board (NRPB) which can advise the government on the safety of tiles. It will also improve the radiological database of the country for future references and benchmarks.

1.6 Limitations of the Study

There were tight timelines for collection, and transportation of the tiles considering that they are heavy matter and with many brands in the market which could not be found in the same town.

Financial constraints in traveling, purchasing, preparation of samples, and analysis were experienced since the study was not sponsored.

The smallest package of ceramic tiles in the market was mostly a packet with 17 pieces and no dealer would accept to sell a single piece from the package as this would affect its value and demand hence being forced to buy a whole packet only to use one piece. This made the sample collection expensive.

1.7 Scope of the Study

This research was done to establish the radiation levels from radio nuclides in ceramic building tiles in Kenya. The tiles were sampled from local companies like Twyford, saj, and Bolgasa and foreign companies like Virony of China Good will of Uganda and Sawa of Tanzania. Thirty-seven sample tiles were collected for the study from different outlets in Nairobi city, Kitui town and Mwingi town which were used to establish the levels of natural radioactivity of ^{232}Th, ^{238}U, ^{40}K in the ceramics.

1.8 Assumptions

i. The Ceramic tiles used in Kenya contain the primordial radio nuclides ^{232}Th, ^{238}U and ^{40}K.

ii. The activity concentrations of; ^{232}Th, ^{238}U and ^{40}K for ceramic building tiles used in Kenya exceeds the world's averages.

iii. Ceramic building tiles used in Kenya are radio logically harmful to human beings.

CHAPTER TWO

2.0 LITERATURE REVIEW

2.1 Introduction.

This section is a presentation of the previous works on the radiation levels of building materials more especially on ceramic and porcelain tiles. Such studies have been done in different parts globally giving substantial data on the levels of human exposure to the radiations and the health effects thereof.

2.2 Radioactivity Studies on Ceramic Tiles Around the World

Radiological analysis of 151 samples of building materials (soil, sand, tiles and cement) was conducted in Tiruvannamalai District, Tamil Nadu in India. These materials were collected from different areas of the district then gamma ray spectrometry was done. The results obtained showed that the highest values of the specific activity concentration of ^{226}Ra, ^{232}Th and ^{40}K were 116.10 for soil, 106.67 for sand and 527.53 for tiles in Bqkg^{-1}, while the lowest observed values of the activity concentration of the same radioisotopes were 35.73, 37.75 and 159.83 for cement in Bqkg^{-1}, respectively. The radiological hazards thereof were determined by calculation of the radium equivalent (Ra_{eq}), the indoor gamma dose rate absorbed (*D*R), annual effective dose rate (AED), the activity utilization index (*I*), alpha index ($I\alpha$), gamma index ($I\gamma$), and the external and internal hazard indices. The estimated average value of the absorbed dose rate was 148.35 nGyh^{-1} which was slightly above the world's average of 60nGy h^{-1} while the annual effective dose was 0.1824 mSvy^{-1} which was lower than the limit recommended. Values of the other hazard indices were all below the thresholds recommended(Raghu *et al.*, 2017).

A radiometric survey to estimate the values of radiation hazard indices from zirconium materials used in ceramic tile industries was done in Bangladesh. Fourteen (14) samples of tiles collected from Chattogram mega port in the country were analyzed using hyper pure germanium detector. The activity concentration of ^{226}Ra recorded for all samples ranged from 21.83±2.67BqKg^{-1} to 515.13±10.45BqKg^{-1}while the average value was 270.75±7.56BqKg^{-1}. The activity concentration of the ^{232}Th in all the samples ranged from 15.67±1.57 to 131.67±4.75BqKg^{-1} with a mean value of 42.99±3.13BqKg^{-1}. The activity

concentration of the ^{40}K in all the samples varied from 12.07±7.70BqKg^{-1} to 90.63±10.43BqKg^{-1} with an average value of 34.48±7.81BqKg^{-1}. Also calculated were the radium equivalent activity, absorbed dose, internal hazard index, external hazard index and the annual effective dose equivalent whose ranges were 45.17 to 705.19BqKg^{-1}, 20.22 to 308.12 out and 24.36 to 369.75nGyh^{-1}in, 0.18 to 3.30, 0.12 to 1.91 and 0.14 to 2.19mSvy^{-1} respectively. Some samples had radium equivalent values higher than the recommended 370BqKg^{-1} and indices higher than the accepted upper limit of a unit 1(Siraz *et al.,* 2023).

Natural radioactivity assessment in building tiles done in Italy showed an activity concentration of ^{226}Ra, ^{232}Th and ^{40}K which ranged as 36-87, 38-86 and 411-996BqKg^{-1}respectively. The radium equivalent activity was between 130-261Bqkg^{-1} for porous ceramic fired tiles. For porcelain tiles, activity concentration of radio nuclides; ^{226}Ra, ^{232}Th and ^{40}K ranged as 20-708, 33-145 and 158-850Bqkg^{-1}respectively. Radium equivalent value for the latter tiles lied between 93-943BqKg^{-1}. This showed that some of the tiles were harmful to human health(Righi & Bruzzi, 2006). The other radiological hazards assessed i.e., the indoor gamma dose rate absorbed, the annual effective dose, alpha index ($I\alpha$), gamma index ($I\gamma$), activity utilization index (I) and the external and internal hazard indices were all below the recommended limits.

Radiation hazard indices for eleven samples of ceramic floor and wall tiles were calculated in Iraq using thallium doped sodium iodide gamma ray spectrometer. The mean activity concentration of ^{238}U was found to be 102.123Bqkg^{-1} for wall tiles and 101.216BqKg^{-1} for the floor tiles. For ^{232}Th the mean activity concentration was 52.410BqKg^{-1} for wall tiles and 87.530BqKg^{-1} for the floor tiles. All this was found to exceed the world's average values. For ^{40}K the average activity concentration was 328.600BqKg^{-1} for wall tiles and 304.566BqKg^{-1} for the floor ceramic tiles, both of which were below the world's mean of 420BqKg^{-1}. The radium equivalent value, the effective dose, external and internal hazard index values were 226.25BqKg^{-1}, 0.24mSvy^{-1}, 0.61, 0.89 respectively. These parameters were below radio logically harmful thresholds (Amana, 2017).

In Belgrade Serbia, activity concentration of ^{238}U, ^{235}U, ^{232}Th, ^{226}Ra and ^{40}K was calculated for sixteen samples of ceramic building tiles that were commercially available. The results reported an activity concentration of ^{226}Ra ranging from 61 to 150BqKg^{-1} in floor tiles, while for wall ceramic tiles the value of activity concentration of ^{226}Ra ranged from 70 to 135BqKg^{-1}. The activity concentration of ^{232}Th ranged from 53BqKg^{-1} to 72BqKg^{-1} and 50BqKg^{-1} to 101 BqKg^{-1} in floor and wall ceramic tiles respectively. For ^{40}K the activity concentration value was found to range between 560 and 1030BqKg^{-1} for floor ceramic tiles and between 590 and 1070BqKg^{-1} for wall tiles. ^{235}U had concentrations between 2.8 and 4.0BqKg^{-1} for floor tiles and between 2.8 and 6.4BqKg^{-1} for wall tiles. For ^{238}U, activity concentrations ranged between 43 and 114BqKg^{-1}(floor tiles) and 43 and 143BqKg^{-1} (wall tiles). These values were below the world recommended limits. The study showed that radioactivity in the sampled building tiles varied depending on the region of origin (Janković *et al.*, 2013).

The natural radioactivity levels for 80 samples of ceramic building tiles were studied in the same country giving a mean activity concentration of the radioisotopes ^{232}Th, ^{238}U and ^{40}K as50±3Bqkg^{-1}, 67±4Bqkg^{-1} and 500±26Bqkg^{-1} respectively. For the 80 samples the radium equivalent ranged from 31±4Bqkg^{-1} (sample from Croatia) to 411±15Bqkg^{-1} (sample from Italy). The values of gamma dose rates, indices and annual effective doses were calculated and found to be within the permissible limits. The results signified no harmful radiation exposure from the building tiles(Nataša *et al*., 2020).

A study was done to establish the natural radioactivity levels in ceramics and cement samples collected in the Riyadh area, Saudi Arabia. The analysis was performed using hyper pure germanium gamma ray detector. The activity concentrations of ^{226}Ra, ^{232}Th, and ^{40}K had ranges from 45.0±4.2 to 177.80±7.50BqKg^{-1}, 49.10±2.60 to 228.40 ±6.80BqKg^{-1}, and 370.00±5.30 to 1269.00±12.20BqKg^{-1} respectively for the ceramic tile samples and from 11.4±2.00 to 28.70 ± 5.30BqKg^{-1}, 8.40±1.30 to 10.80± 1.10BqKg^{-1}and 50.70±2.10 to 209.70±3.50BqKg^{-1} respectively for the samples of cement. These values obtained were used in calculations to determine the radium equivalent activity, external hazard index, absorbed dose and annual effective dose rate which were found to be

299.40±94.80BqKg^{-1}, 0.30, 138±42.40nGyh^{-1} and 0.68±0.21mSvy^{-1} respectively for the ceramic samples and for the samples of cement, the values were 36.8±7.74BqKg^{-1}, 0.12±0.02, 20.35±4.39nGyh^{-1} and 0.10± 0.02mSvy^{-1}, respectively. The cement samples posted radiological parameters all within the safety limits. A few of the ceramic samples had exceeded the world's radium equivalent limit (370BqKg^{-1}) and also the hazard index of a unit (Hameed *et al.*,2021).

Another study was done in the same country to determine the chemical composition and the natural radioactivity levels in ceramic tiles for interior decorations and constructions. Twenty-one (21) elements were confirmed present in the tiles whereby Calcium, Silicon, iron, sodium, Aluminum, Magnesium and potassium were the major elements. Heavy metals like Manganese, Chromium, Cobalt, Nickel, Copper, Zinc, Cadmium and lead were also detected but as traces. Activity concentrations of ^{238}U (^{226}Ra), ^{232}Th and ^{40}K were found to range between 29-129, 32-114 and 83-1100BqKg^{-1} respectively (Alghamdi & Almugren, 2019).

The levels of natural radioactivity in ceramic building tiles and the associated radiological hazard parameters were studied using a high purity germanium detector in Turkey. The average activity concentration of the primordial radioisotopes (^{232}Th, ^{238}U &^{40}K) was found to be 51.23± 2.18, 36.58± 2.64 and 420.81±12.87BqKg^{-1} respectively. These registered values were lower than the world's mean except for ^{232}Th which was higher by 28.23BqKg^{-1}. The values of the radiological hazard parameters like radium equivalent activity, absorbed dose, annual effective doses and hazard indices recorded were all lower than the world's averages. The study showed that the tiles could be used safely with no significant radiological hazard in constructions (Dizman *et al.*, 2019).

Activity concentration of the radioisotopes (^{226}Ra, ^{232}Th and ^{40}K) for 15 types of ceramic tile samples used in Nigerian houses were studied using Hyper pure Germanium gamma radiation detector. The average activity concentrations of the radio nuclides; ^{226}Ra, ^{232}Th, and ^{40}K were found to be 61.1±5.5Bqkg^{-1}, 70.2±6.08 BqKg^{-1} and 514.7±59.8BqKg^{-1} respectively. From the study, average values of radium equivalent, absorbed dose rate,

external and internal hazard index, annual effective dose, Gamma activity Index (I_γ) and Alpha Activity Index (I_α) were: 204.42BqKg^{-1}, 177.61nGyh^{-1}, 0.55, 0.77, 0.96 mSvy^{-1}, 0.74 and 0.32 respectively (Joel *et al.,* 2018). The mean radium equivalent value registered was less than 370BqKg^{-1} which is the recommended limit value, but the mean values for other radiological hazards for some samples were slightly higher than world's recommended values except for internal hazard index ($H_{in)}$, external hazard index ($H_{ex)}$ and the annual effective dose (AED) which were within the international reference value of a unit.

Another research was done in Nigeria to evaluate the activity concentration of natural radio nuclides (^{226}Ra, ^{232}Th and ^{40}K) for ceramic wall and floor tiles using hyper pure germanium gamma ray detector. The values of activity concentrations of the radioisotopes ^{226}Ra, ^{232}Th and ^{40}K were found to range from 52.00 ± 2.0 to 105.00 ± 3.0, 56.00±1.0 to 115.00±2.0 and 185.00±9.0 to 893.00±17BqKg^{-1} with average values of 72.00 ± 14, 84.00 ± 18 and 629.00±198BqKg^{-1} respectively for the wall ceramic tiles. For floor tiles, the values of activity concentrations of ^{226}Ra, ^{232}Th and ^{40}K ranged from 41.00±2.0 to 131.00±4.00, 59.00±1.0 to 127.00±2.0 and 351.00 ± 11 to 979.00±16BqKg^{-1} with average values of 74.00±31, 82.00±24 and 618.00 ± 231Bqkg^{-1}, respectively (Ademola, 2009).

Radiological hazard effects for 16 samples of local and imported ceramic tiles were done in Egypt using hyper pure germanium detector (HPGe). The average activity concentration of the radioisotopes; ^{226}Ra, ^{232}Thand ^{40}K were 47.4±3.3, 42.84±2.8 and 313.6±34.3BqKg^{-1} respectively. The other radiological parameters like radium equivalent, absorbed dose, internal hazard index, external hazard index and annual effective dose rate were 131.51BqKg^{-1}, 14.49nGyh^{-1}, 0.49, 0.36 and 0.07msvy^{-1} respectively. All these were below the thresholds recommended in the ICRP reports. The tiles were therefore confirmed radio logically suitable for use in construction (Uosif *et al.,* 2015).

A study was done in Sudan to compare the natural radioactivity levels and the radiological parameters for some imported ceramic tiles. Twenty-five samples were collected and analyzed using sodium iodide gamma ray spectrometry system, the average values of activity concentration for ^{238}U, ^{232}Th and ^{40}K was 183±70, 51±44 and 238±77BqKg^{-1}

respectively(Saif *et al.*,2022).The study posted a mean radium equivalent value of 274±106BqKg^{-1} which was below 370BqKg^{-1} (recommended limit). The absorbed dose (D), the annual effective dose (AED) and the external hazard index (Hex) were found to be 125±48nGyh^{-1}, 1.23±0.48mSvy^{-1} and 0.74±0.29 respectively. The value of D was far above the threshold, but the indices were within the world's average limits. Generally, the imported tiles had higher radioactivity levels than the locally manufactured. The locally manufactured therefore were safer for human handling.

In Sudan, a survey of the levels of natural radioactivity in selected building materials was done in 2020. For the study 52 building material samples including ceramic tiles, cements, red clay bricks and porcelain ware were prepared. Analysis was done using a high purity germanium detector (HPGe). It was observed that the average activity concentration of radio nuclides; (^{226}Ra, ^{232}Th, and ^{40}K) ranges were 12–40, 10–70, and 28–94BqKg^{-1} respectively. For cement alone, the activity ranges of the three radio nuclides were 10–35, 12–28, and 87-143BqKg^{-1} respectively while in cement blocks it was 32–132, 26–87, and 285–1070BqKg^{-1} respectively. In porcelain and ceramic tiles the values were 8-527, 18–118 and 129–812BqKg^{-1} respectively. The absorbed dose rates in air ranges were 12.00±3.0 to 40.50±23.0nGyh^{-1} for materials which were used in a superficial quantity and 34.40±8.9 to 173.30±52.0nGyh^{-1} for materials which were used in bulk. The annual effective doses varied from 0.06 to 0.85mSvy^{-1}. The values for the hazard indices, radium equivalent and annual effective dose were within the recommended thresholds limits(Adreani *et al.*, 2020).

A study was done in 2022 to determine the radiation levels in construction tiles used in Bungoma County-Kenya. Twenty (20) samples for both local and imported tiles were collected from the area and prepared for analysis. Thallium doped sodium iodide gamma ray spectrometer was employed in the analysis. The minimum values of activity concentration for ^{232}Th, ^{238}U and ^{40}K were found to be 52±2.62Bqkg^{-1}, 6±0.32 BqKg^{-1} and 1165±58.29BqKg^{-1} while the maximum values were 254±12.7BqKg^{-1}, 31±1.57BqKg^{-1} and 2193±109.65BqKg^{-1} respectively. The mean activity for ^{238}U, ^{232}Th, and ^{40}K obtained were 109±5.48BqKg^{-1}, 11±0.55BqKg^{-1} and 1574±78.7BqKg^{-1}respectively. The activity

concentration of ^{232}Th and ^{40}K exceeded the world's agreed average values of 45BqKg^{-1} and 420BqKg^{-1} respectively. The activity concentration of ^{238}U evaluated was lower than the world's average of 33BqKg^{-1}. The mean absorbed dose rate was 140±7.03nGyh^{-1} which was higher than the world's average value of 60nGyh^{-1}. The average value of radium equivalent obtained was 288±14.44 BqKg^{-1} which is lower than the recommended limit of 370BqKg^{-1}. Internal and external hazard indices were found to be 0.80±0.04mSvy^{-1} and 0.70±0.03mSvy^{-1} respectively (Nalianya *et al.,* 2022). Considering that this study was carried out using few samples and from only one region in the country, it may not have been fully representative of the radiation doses. This prompts more and broader surveys on the radiation levels of the building tiles in the country.

Various studies have been carried out for different construction materials in different regions of the world showing different levels of radioactivity. These levels vary from region to region depending on the geological composition of the region. In Kenya there is only one documented study done on the ceramic tiles. Therefore, this research was significant to determine the level of natural radioactivity for ^{238}U, ^{232}Th and ^{40}K in the ceramic building tiles used in Kenya and assess their radiological hazards on human beings.

CHAPTER THREE

3.0 THEORETICAL BACKGROUND

3.1 Introduction

This chapter is a discussion of the concepts of radioactivity, types of radioactive emissions and their properties. It explains the interaction of different radiations with matter and the diametric quantities used in the measurement of the doses. It also discusses the working of the gamma ray spectrometer and particularly the sodium iodide scintillator counter which was used in this study.

3.2 Types of Radiations

Radiation is the flow of atomic and subatomic particles and waves transferring energy through a medium. This medium can be air, water, a solid or even vacuum. There are two radiation categories, that is non-ionizing and ionizing radiations as shown in figure 3.1.

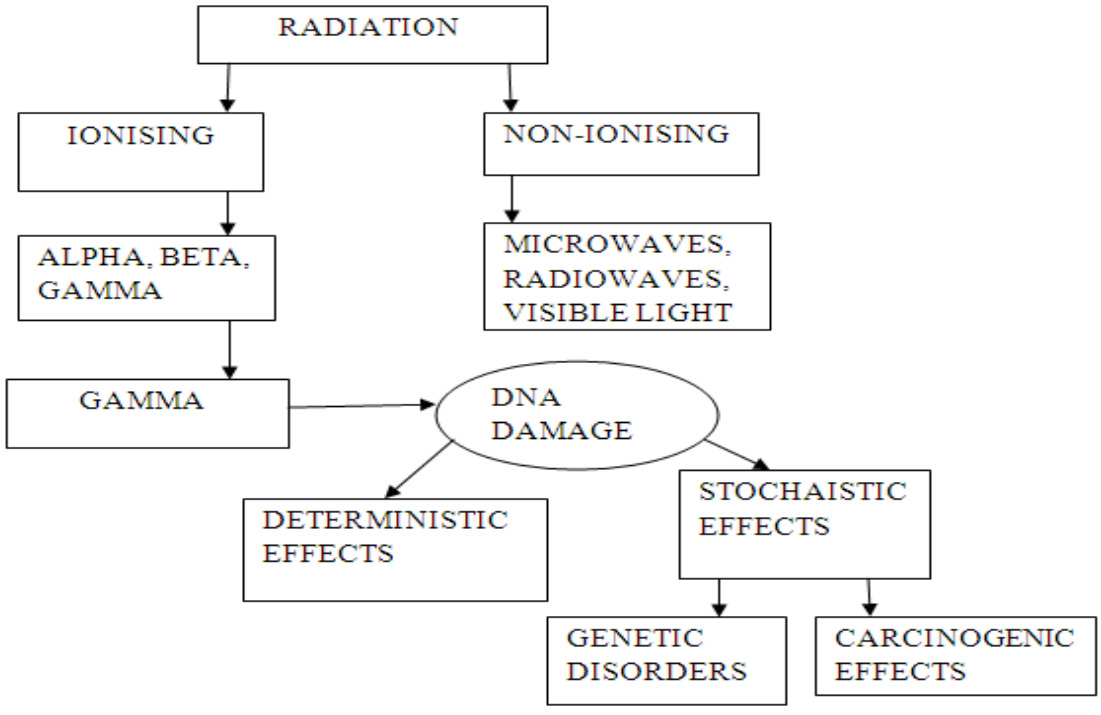

Figure 3.1: Non-ionizing and Ionizing Radiations

Non-ionizing radiation is that which has a small amount of energy such that it cannot ionize matter. It is inclusive of visible light, ultraviolet, and nearly all types of laser light, infrared

and microwaves. It is unable to strike and dislodge electrons from atomic energy levels. On the other hand, ionizing radiation is that which has enough energy to create ion pairs in atoms. It is the major concern of the nuclear regulatory authority (NRA) of any country. It acts by knocking electrons off atoms and molecules of matter through which they pass. These electrons create many unstable radicals which generate indiscriminate chemical reactions around them. This alters shapes of molecules composing the cells of the human body denaturing or killing the cells leading to ill health or even death.

The effect of radiation on a living cell is dependent on type, amount and rate of absorption. An ionizing radiation interacting with the human body can strike the DNA causing its discontinuity or breakage. In an attempt to self-repair the breakage, mistakes may occur resulting in genetic abnormality of the cells known as mutation. Developments of such deformed cells are responsible for some forms of cancer. Skin burns and cataracts are also among the hazards of ionizing radiation. Some examples of these radiations include neutrons, alpha particles, beta particles, x-rays, and also gamma rays (Kharisov & Kharissova, 2013).

3.2.1 Neutrons

Neutrons are neutral particles whose mass is slightly bigger than that of a proton. Since they are neutral, their ionizations are indirect. In biological matter, these particles do eject protons from atomic nuclei via nuclear collisions. The ejected protons which are charged can then ionize bio matter directly.

3.2.2 Alpha Particles

They are massive heavily positively charged particles. They are equivalent to helium ions and are classified as high linear energy transfer (LET) particles which interact to deposit the energy they have over a small volume of matter. Alpha particles are a result of the radioactive disintegration of heavy elements like uranium, plutonium, radium and thorium. Because of their duo-positive charge and massive size, they have greater ionizing ability, but their big masses result in low velocity and therefore little penetration. Alpha particles of energy from 4 - 10 MeV have ranges of about 5–11 cm in

air. Their corresponding penetration ranges in water is from 20 to 100 μm. They thus cause more harm to fewer cells since they ionize many atoms within a short range. The nuclear equation 3.1 shows an alpha decay of uranium-235 to thorium-231.

$$^{235}_{92}U \longrightarrow {}^{4}_{2}He + {}^{231}_{90}Th \quad \ldots\ldots 3.1$$

In air the alpha particle will lose its energy as it collides with particles in its flight path. Figure 2.2 shows how an alpha particle loses its energy as it penetrates air.

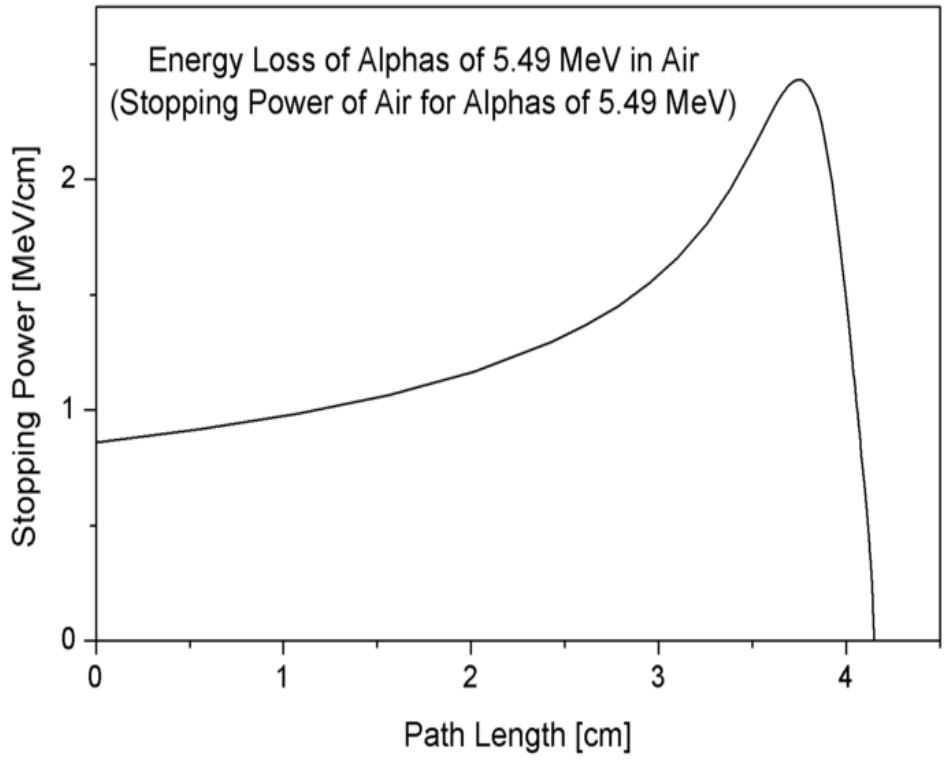

Figure 3.2: A Curve Showing the Energy Attenuation of an Alpha Particle in Air.(Gilmore, 2008).

3.2.3 Beta Particles

A beta particle is a high energy, high speed electron (β^-) or positron (β^+) ejected from the nucleus of a radio nuclide. It has a net charge of negative or positive one. These particles directly interact with vital biological macromolecules such as DNA, RNA, proteins and enzymes ionizing them. They are majorly electrons but result from radioactive disintegration of unstable atoms. Beta particles are emitted with indiscrete energy ranges

up to a maximum which is characteristic of an individual radionuclide. Their range in air is much greater than that of alpha particles hence higher penetrating power. However, their ionizing potential is much less than that of alpha particles. Equation 3.2 represents the emission of a beta particle during the disintegration of carbon-14 to nitrogen-14.

$$^{14}_{6}C \longrightarrow {}^{14}_{7}N + {}^{0}_{-1}e \ldots\ldots\ldots\ldots\ldots\ldots\ldots\ldots\ldots\ldots\ldots\ldots\ldots\ldots 3.2$$

3.2.4 X-Rays

They are neutral highly energetic radiations which are generally produced when fast moving electrons are suddenly stopped by a metallic target. The energy content in X-rays is large enough to break the deoxyribose nucleic acid (DNA) directly or ionize water molecules to hydrogen (H^+) and hydroxyl (OH^-) ions (Knapp, 2013). These free ions and radicals create a series of chemical reactions resulting in breaking of the macromolecule's chemical bonds forming abnormal structures. Depending on the extent of damage the cells can self-repair or die. In case of imperfections in the repair, the weakness can be copied to more cells which can lead to some cancer forms. In case such cells deal with transmission of hereditary details then there will be a likelihood of hereditary disorders to the descendants(UNSCEAR, 2000). In smaller amounts, X-rays are used for medical imaging tests, food irradiation, cancer treatment, and airport security scanners. They were not the focus of this study because their general method of production is by accelerated electrons striking a metallic target which is not radioactivity.

3.2.5 Gamma Rays

This is a highly energetic radiation whose symbol is γ. It is the highest penetrating form of e.m radiation which results from radioactive breakdown of unstable atomic nuclei. It has the highest frequency hence the shortest wavelength of all the electromagnetic waves. As seen in equation 3.3, gamma rays have neither mass nor charge and may accompany the emission of other particles like alpha and beta.

$$^{222}_{86}Rd \longrightarrow {}^{218}_{84}Po + {}^{0}_{0}\gamma + {}^{4}_{2}He \ldots\ldots\ldots\ldots\ldots\ldots\ldots\ldots\ldots\ldots\ldots\ldots\ldots\ldots 3.3$$

Radon-222 in the equation 3.3 breaks down to polonium-218 releasing an alpha particle and a characteristic gamma radiation. Gamma ray interaction with matter causes a radiation

field with negative electrons and positive ions. A particle of zero rest mass like a gamma photon has its kinetic energy (KE) given by equation 3.4

$$E = h\nu = \frac{hc}{\lambda} \ldots\ldots\ldots\ldots\ldots\ldots\ldots\ldots\ldots\ldots\ldots\ldots\ldots\ldots\ldots\ldots\ldots\ldots\ldots\ldots\ldots\ldots 3.4$$

Where,

h is plank's constant, ν is the gamma ray photon frequency, C is the speed of light ($3x10^{10}cms^{-1}$), and λ is the radiation wavelength.

Their high energy and small size cause deeper penetration and less damage per interaction. They are thus said to have low "Linear Energy Transfer" (LET). If a Gamma ray has its energy greater than 10 MeV, the human body will be transparent to it and it experiences less harm from the ray. Gamma-rays accompany other decays and are released as the characteristic radiation energy when the corresponding excited atoms try to attain their ground state as in Figure 3.4.

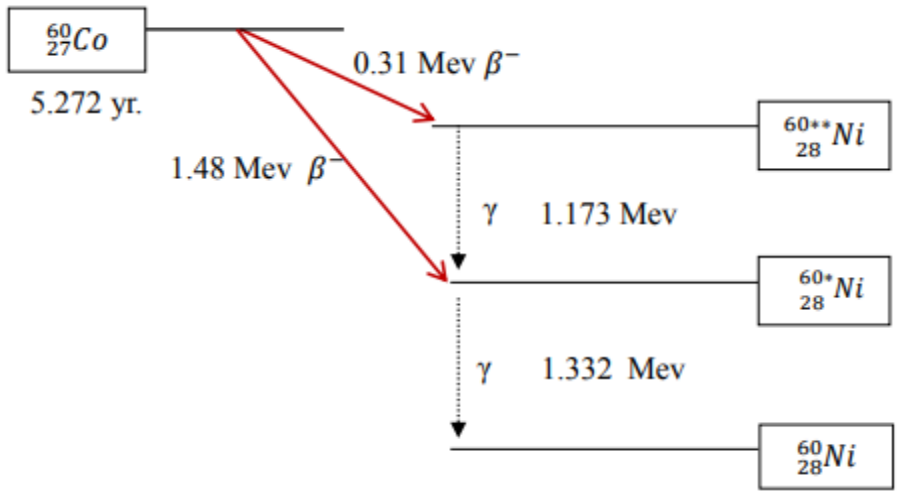

Figure 3.3: Decay series of Co-60. It undergoes beta decay to an excited *N*i-60 (Knipp & Uhlenbeck, 1936).

In this decay series, 99.88% of ^{60}Co undergoes beta decay to an excited ^{60}Ni emitting an electron whose energy is 0.31Mev together with an antineutrino. The ^{60}Ni then drops to its ground state by emitting two gamma rays of energy 1.173Mev and 1.332Mev respectively. 0.12% of the ^{60}Co decays by emitting a beta particle of 1.48Mev to an excited ^{60}Ni which

releases a gamma ray of energy 1.332Mev as it falls to its ground state. The intensity and energy content of gamma radiation determines the hazardous effect it can bring to bio matter. The higher the intensity of the radiation the more the number of affected cells while the higher the energy content of the radiation then the greater the cell damage.

Gamma rays can strike and harm the DNA directly or indirectly as shown in Figure 3.4

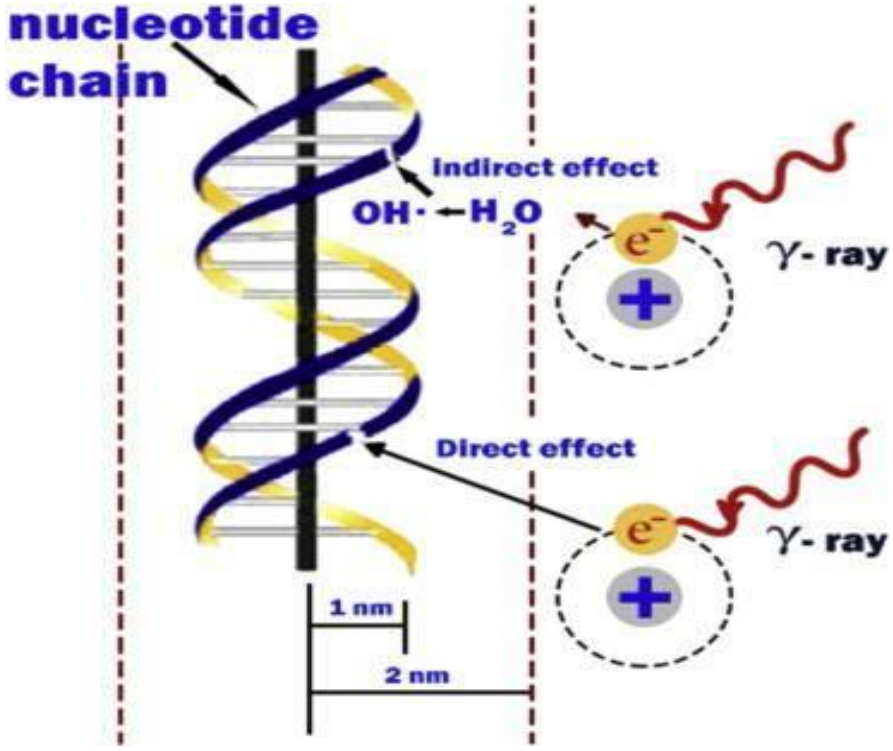

Figure 3.4: Direct and indirect interaction of a gamma ray with a nucleotide(Desouky *et al.*, 2015)

The ionizing radiation can either strike the DNA denaturing it or ionize water molecules creating radicals whose chemical reactions with the DNA distorts its structure.

The various ionizing radiations have different speeds in matter, energy content and ionizing properties. The table 3.1 below is a comparison for alpha, beta, gamma and x-rays.

Table 3.1.Speed, energy and relative ionizing ability of some radiations.

	Speed	**Average Energy**	**Relative Ionizing ability**
Alpha	15,000,000m/s	5MeV	High
Beta	close to speed of light	High (varies hugely)	Medium
X rays	300,000,000m/s	Very high and variable	Low
Gamma	300,000,000m/s	Very high (again, varies hugely)	Low

3.3 Radiation interaction with matter

Gamma radiation was the major focus in this study. This radiation interaction with matter primarily takes place in three modes i.e., photoelectric effect, Compton scattering and electron-positron pair production depending on the energy content of the photons. On striking matter, the radiation beam intensity may be attenuated, it may undergo total absorption or may be scattered by the matter (Knoll, 2010).

3.3.1 Photoelectric effect

It is also known as photoelectric absorption. In this case a gamma photon of low energy (energy $\leq$ 200KeV) interacts with an orbital electron in any of the bound shells of the atom. The electron receives kinetic energy (K.E) enough to have it knocked off from the orbital. All the incident photon energy is deposited in the detector material. Figure 3.5 illustrates photoelectric absorption

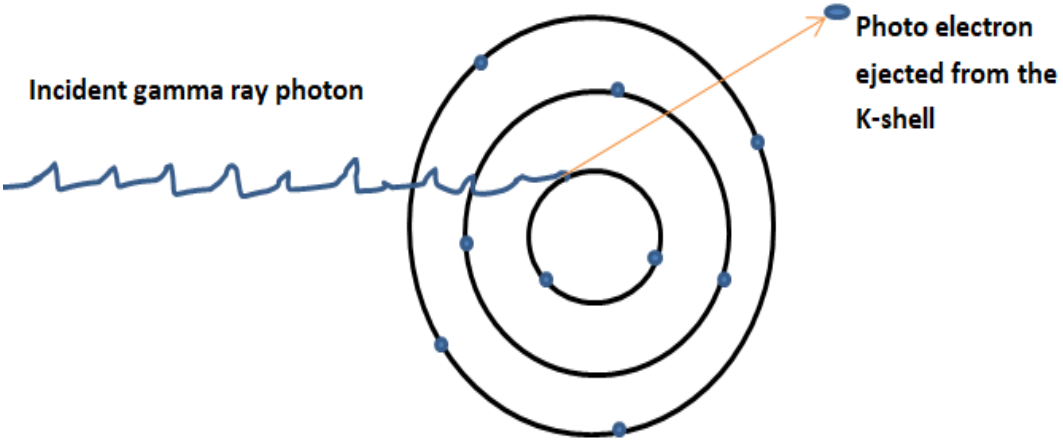

Figure 3.5: Photoelectric effect (Matsitsi, 2020)

The atom is left excited and may attain equilibrium by distributing the excitation energy to the remaining electrons. It can also have a higher level electron dropping down to the vacancy left by the dislodged electron through X- ray fluorescence. The K.E of the liberated electron is the energy difference between the incident gamma ray photon and the electron's binding energy in its original level given by equation 3.5 (Gilmore, 2008).

$$E_e = h_v - E_b \ldots\ldots\ldots\ldots\ldots\ldots\ldots\ldots\ldots\ldots\ldots\ldots\ldots\ldots\ldots\ldots\ldots\ldots 3.5$$

Where,

E_e is the kinetic energy of dislodged electron,

hv is the incident gamma ray energy and

E_b is the binding energy of the liberated electron when in its original shell.

3.3.2 Compton Scattering

In this case the incoming photon at a minimum energy of about 0.25MeV strikes an electron in one of the atomic outer shells. The photon is scattered as in figure 3.6. The energy of the incident photon is shared between the recoil electron and the scattered ray. The energies after interaction are dependent on the incidence angle Φ (angle between the original photon direction and the scattered photon) (Knoll, 2010). If it brings about a reduction in energy (wavelength increase) of the incident photon then it is known as Compton Effect.

Inverse Compton scattering on the other hand occurs if a charged particle transfers its energy to the incoming photon. Compton scattering shown in figure 3.6 is the most common process of gamma ray interaction with matter.

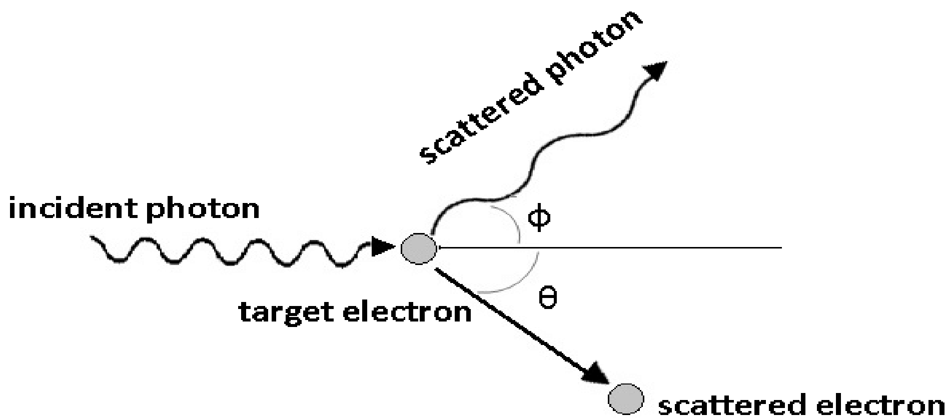

Figure 3.6: Compton Scattering(Venugopal & Bhagdikar, 2012)

The amount by which the incident photon's wavelength changes, is known as Compton shift. The energy E_o of the scattered electron is given by the equation 3.6

$$E_0 = E - E' \quad \ldots 3.6$$

Where,

E is energy of the gamma ray photon

E' is the energy of the scattered photon

The direction of the scattered electron and also the scattered gamma ray depends on the energy given to the electron on interaction (Odumo, 2021). The ratio of scattered photon energy to incident photon energy is given by equation 3.7. (Gilmore, 2008)

$$\frac{E'}{E} = \frac{1}{1 + (1 - cos\phi)E/m_e c^2} \quad \ldots 3.7$$

Where,

$m_e c^2$ is the electron's rest energy.

Φ is the angle between the incident and the scattered gamma photons (scattering angle)

The minimum scattered energy E′ occurs when $\phi = 180^0$ and the scattered electron moves along the direction of the incident gamma photon. When $\phi = 0$ the photon does not lose any energy and thus the recoiling electron does not gain any energy.

3.3.3 Positron-Electron Pair Production

In this case an incident photon strikes an atom and its energy is converted to matter. The incoming photon has high energy (approximately 1.022MeV and above) and annihilates within the electric field around the atomic nucleus forming an electron and a positron as in Figure 3.7. For gamma photons with high energy, pair production is the dominant process of gamma ray interaction with matter(Ragheb, 2011). This does not affect orbital electrons but occurs near the nucleus of the atom as shown in Figure 3.7.

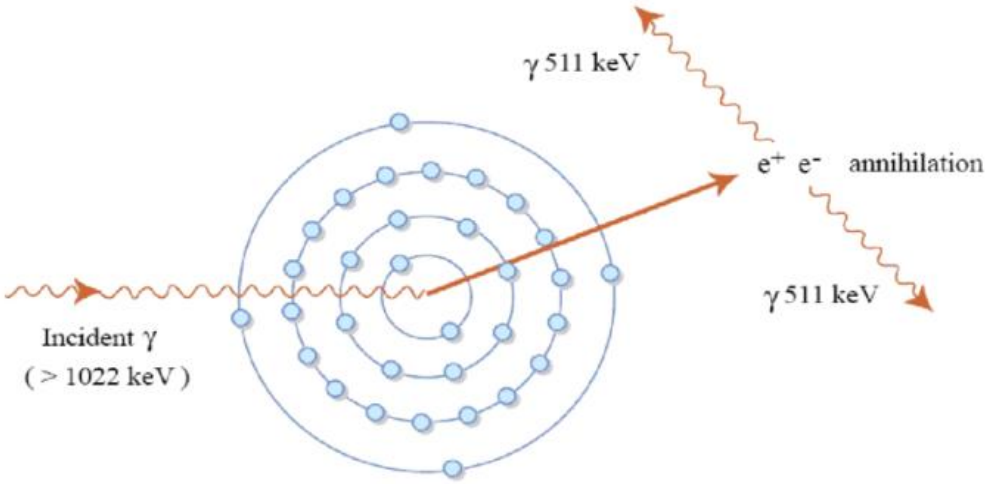

Figure 3.7: Electron-Positron Pair Production(Ali, *et al.*, 2019)

For a photon with energy above 1.022MeV, the extra energy is shared between the electron and the positron as K.E.ie

$$h\upsilon = m_e c^2 + E_{KE}^{-} + E_{KE}^{+} \ldots\ldots\ldots\ldots\ldots\ldots\ldots\ldots\ldots\ldots\ldots\ldots\ldots 3.8$$

The nucleus remains almost the same since it receives very little energy. The electron and the positron combine in the annihilation process after loss of K.E. to form two gamma rays of energies 0.511Mev(Steinhauser & Buchtela, 2012).The probability of the electron–positron pair production is dependent on the atomic number Z, being bigger in atoms with high atomic numbers.

3.4 Principles of the Gamma Ray Spectrometer

Gamma ray spectroscopy refers to the science of identification and quantification of radio nuclides by analysis of the gamma ray spectrum which is produced by a spectrometer. Gamma rays have the highest energy of all the electromagnetic waves because of their short wavelength. The energy they carry is given by the equation 3.9

$$E = \frac{hc}{\lambda} = h\upsilon \ldots\ldots\ldots\ldots\ldots\ldots\ldots\ldots\ldots\ldots\ldots\ldots\ldots\ldots\ldots\ldots\ldots\ldots 3.9$$

Where, E is the incident gamma photon's energy,

h is plank's constant($6.626x10^{-34}m^2kgs^{-1}$)

c is the speed of light ($3x10^{10}cms^{-1}$)

$\boldsymbol{\lambda}$ is wavelength and

υ is frequency of the radiation

Radio nuclides mostly emit gamma rays of energy ranging from a few Kev to 10 Mev. The major components of the gamma ray spectrometer are shown in the figure 3.8.

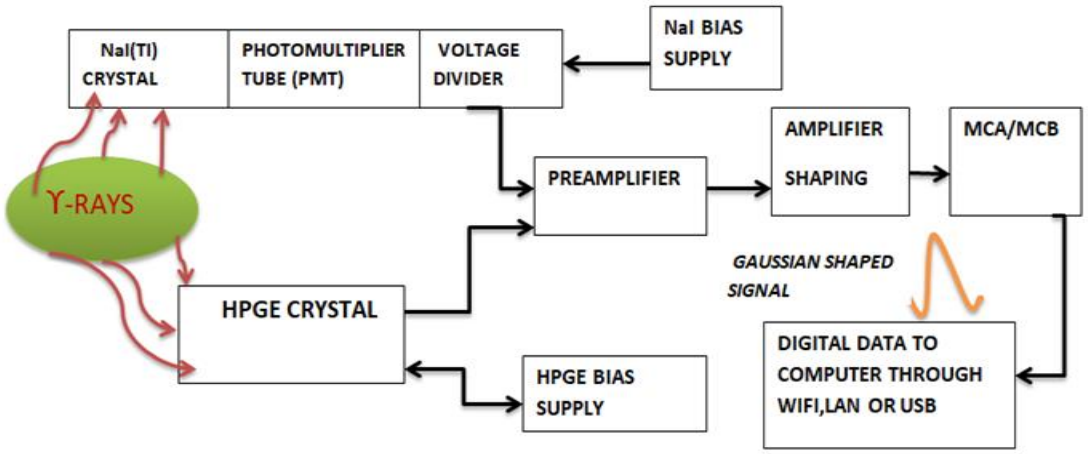

Figure 3.8: Basic Gamma Ray Detection System.

The system has a radiation detector which is energy sensitive, electronics which are used in processing of the detected signals, such as the multichannel analyzer (MCA), amplifiers and data read out devices which generate, exhibit and store the spectra. Commonly used detectors are the sodium iodide scintillation counters NaI (TI) and the high purity germanium (HPGE) detectors as seen in the chart. The detector waits for the gamma ray

interaction to occur in its detector volume, this happens by photoelectric effect, Compton scattering and electron-positron pair production. Photoelectric absorption is commonly preferred because all the energy of the incident photon is absorbed and therefore it gives a stronger response.

The pulse of voltage produced by the detector (photo multiplier) in the scintillation counter is then shaped by the multichannel analyzer/buffer (MCA/MCB).The MCA takes very small amount of voltage signal which is produced by the detector then shapes it into a Gaussian or trapezoidal form and converts it to a digital signal. There is an analogue to digital converter (ADC) which sorts out the pulses according to their height. This ADC has a specific number of channels/bins into which the pulses are sorted.

The MCA output is sent to a computer via a USB, LAN OR WIFI. The computer then can store, display and analyze the data. There are various software packages from different manufacturers for spectra analysis, energy calibration, peak and net area calculation and also resolution calculation.

3.4.1 Detector Resolution

The detector energy resolution (Re) is the measure of its ability to distinguish gamma rays with close energies. A good resolution means that the detector can separate different energy peaks easily. This helps to identify different radio nuclides in the spectrum. Commonly, detector resolution is expressed as the full width at half maximum (FWHM) value on the peak distribution. This is the gamma ray peak width at half of the highest point.

The resolution of a detector can be expressed in absolute (eV) electron volts or in relative terms e.g. a sodium iodide detector may have a FWHM of 9.15Kev at 122Kev.
In relative terms the resolution is given by equation 3.10.

$$Re = \frac{FWHM}{E}\% \ldots\ldots\ldots\ldots\ldots\ldots\ldots\ldots\ldots\ldots 3.10$$

Where, E is the gamma ray energy e.g. the Re can be given as 7.5% at 122 Kev.

3.4.2 Detector Efficiency

The probability that the emitted gamma rays from a source will interact with the detector material and produce a response is the detector efficiency. It is given by the ratio of the detected events per gamma rays emitted. It is also defined as the measure of the amount of radiation that a given detector registers from the overall yield coming from a source. It varies with the volume and the detector material shape, absorption cross-section in the material, the number of attenuation layers that are in front of the detector and the source to detector separation distance. Below are different types of efficiency.

3.4.2.1Absolute Efficiency

It is a ratio of the counts registered by the detector to the total number of gamma rays emitted by the source in all directions. Absolute efficiency is given by equation 3.11.

$$E_{abs} = \frac{Nc}{Ns} \quad \ldots 3.11$$

Where, E_{abs} is the absolute efficiency, Nc is the net count rate (number of pulses recorded) and Ns is the number of radiation quanta emitted by the source.

3.4.2.2 Intrinsic Efficiency

It is the ratio of the total number of events recorded by the detector to the total number of gamma rays striking the detector. It is given by equation 3.12.

$$Intrinsic\ efficiency = \frac{Number\ of\ counted\ photons}{Number\ of\ photons\ entered\ to\ detector} \quad \ldots 3.12$$

3.4.2.3 Full Energy Peak (photo peak) Efficiency

It is the efficiency needed for producing only full energy peak pulses, rather than pulses of any size for the gamma photon.

3.5 Radiation Field Quantities

3.5.1 Energy Fluence

This refers to the energy incident on a given surface per unit area. That is:

$$\psi = \frac{dE}{dA} \quad \ldots 3.13$$

Where dE is the radiation energy incident on a sphere of cross-sectional area dA
Energy fluence is measured in JM^{-2}

3.5.2 Particle Fluence

Refers to the number ofparticles incident on a surface per unit area. It is given by the equation 3.14.

$$\Phi = \frac{dN}{dA} \dots\dots\dots\dots\dots\dots\dots\dots\dots\dots\dots\dots\dots\dots\dots\dots\dots\dots\dots\dots\dots\dots\dots\dots\dots\dots 3.14$$

Where, dN is the number of incident particles on a sphere of cross sectional dA.

3.6 Kinetic Energy Released per Unit Mass (KERMA)

The energy given to electrons by photons may be determined through collision interactions and radioactive interactions. KERMA refers to the sum of the initial kinetic energies of all the charged particles produced by the uncharged ionizing radiation.

$$K = \frac{d\bar{E}_{tr}}{dm} \dots\dots\dots\dots\dots\dots\dots\dots\dots\dots\dots\dots\dots\dots\dots\dots\dots\dots\dots\dots\dots\dots\dots\dots\dots\dots .3.15$$

Where $d\bar{E}_{tr}$ is the mean kinetic energy deposited on the charged particles from uncharged particles in mass dm of a material. Total KERMA ($K_{total)}$ can be split into two parts: collision KERMA (K_{coll}) and radiative KERMA (K_{rad}). Collision kerma refers to the expectation value of the net energy transferred to the charged particles per unit mass at the point of interest, excluding both the radiative energy loss and the energy passed from one charged particle to another. Radiative KERMA refers to the part of KERMA that leads to the production of radiative photons, as the secondary charged particles slow down and interact in the medium. Therefore, the total KERMA can be given by equation 3.16.

$$K_{total} = K_{coll} + K_{rad} \dots\dots\dots\dots\dots\dots\dots\dots\dots\dots\dots\dots\dots\dots\dots\dots\dots\dots\dots\dots\dots\dots\dots\dots\dots\dots .3.16$$

KERMA is measured in gray (Gy)

3.7 Secular Equilibrium

This is a condition in radioactivity whereby the rate of disintegration of a parent nuclide is equal to that of its daughter particle. It happens only if the parent's half-life is much longer compared to that of the daughter such that there is insignificant decay during the time

interval of interest. If the samples are left undisturbed for a long period of time, the decay rate of the parent radionuclide and hence the rate of formation of the daughter radionuclide becomes constant. This is so because the time lapse considered is very minute compared to the half-life of the parent radionuclide. Under this equilibrium, each of the decay chain members has the same activity since the quantity of the daughter radio nuclides builds up until the number of its atoms decaying per unit time equals the number being produced. In this case, the activity of the daughter radionuclide can be determined by the activity of the parent radionuclide. By taking N_D and N_P as the number of atoms of the daughter and the parent radionuclide initially, and the corresponding activities A_D and A_P respectively, the secular equilibrium idea can be explained using decay lawsas given by equation 3.17 (Gilmore, 2008).

$$\frac{dN_D}{dt} = \lambda_P N_P - \lambda_D N_D \quad \ldots\ldots\ldots\ldots\ldots\ldots\ldots\ldots\ldots\ldots\ldots\ldots\ldots\ldots\ldots\ldots 3.17$$

Where λ_P and λ_D are decay constants of the parent and the daughter respectively (McNaught & Wilkinson, 1997).

CHAPTER FOUR

4.0 METHODOLOGY

4.1 Introduction

To ensure quality survey, various equipment/apparatus, processes, experimental procedures and formulae were applied during sample collection, preparation and data analysis. Building tile samples from various local manufacturing companies and imported ones were selected for the study. Collection of samples was done from local outlets in different Kenyan towns including Nairobi city, Kitui town and Mwingi town. The following sections discuss step by step procedures and methods used for data collection, preparation and the experimental setup of the study.

4.2 Materials

The following materials were used in sample collection, preparation and data analysis; A mobile phone for taking photographs, Ceramic floor and wall tiles, Three rectangular carton for ferrying the tiles, a mark pen, labeling stickers,50 ml plastic containers to hold the tile powder, a pulverizer for crushing the tiles to powder, hot air oven for drying the tiles, a 1.0mm mesh sieve, a packaging tape, an electronic weighing balance, IAEA certified reference samples(RG-series),a packet of aluminum foil, Sodium Iodide NaI(TI) gamma ray spectrometer, a computer with data acquisition and analysis software.

4.3 Sample Collection

Sample tiles were purchased from different outlets in Mwingi town Kitui town and Nairobi city. Random sampling method was used to collect thirty-seven (37) tile samples. A total of sixteen (16) samples were from local manufacturers while twenty-one (21) samples were imported from countries such as Tanzania, Uganda, India, and China. The choice of either floor or wall tiles to sample depended on availability in the market.

4.4 Sample Preparation

The tile brands sampled were separately broken down using a mallet and about 500g of each sample wound in aluminum foil. These course samples werepulverized at the Ministry

of Mining and Petroleum Laboratory in Nairobi using the electronic pulverizer shown in figure 4.1.

Figure 4.1: The Crushing Machine used at the Ministry of Mining and Petroleum Headquarters, Nairobi-Kenya (Open)

A 1.0mm mesh sieve was used to sieve the tile powder to ensure homogeneity of the powder particles. The fine power from each of the tile brand was packaged in aluminum foil papers in preparation for drying. The samples were subjected to a temperature of 120^0C for two hours in a hot air oven to get rid of all moisture as shown in Figure 4.2.

Figure 4.2: Tile Powder Samples Being Fed into the Hot Air Oven for Drying at South Eastern Kenya University.

From each of the tile dry powder a mass of 203g sample equivalent to the mass of the reference sample was accurately measured using the electronic weighing balance and then placed into an airtight plastic container. The samples were stored in a dry environment for 28 days to ensure secular equilibrium is attained. All these containers were completely sealed with masking tape and labeled with codes running as KX01.

- The first alphabet represented the country of origin.
- The second alphabet is the manufacturer company.
- The last numeral is the brand number e.g.KX02 stands for tile brand number two manufactured by company X in country K.

4.5 Sample Analysis Using Gamma-Ray Spectroscopy

Analysis of the samples was done using thallium doped sodium iodide detector (NaI (TI)) to identify gamma radiation emitters in the tiles and establish the energy content thereof.

This detector was preferred due to itslow dead time and high efficiency in radiation detection even though it has low spectra resolution. The detector also has low maintenance costs as it doesn't require cooling unlike some detectors used in gamma radiation measurements.

4.5.1 Energy Calibration

This is the assigning of energy values to the channel numbers of the detector. It ensures that one can correctly identify the energy peaks representing certain radio nuclides by the corresponding centroid energy (Gilmore, 2008). Before actual counting began, the detector calibration was performed using the standard point sources from the International Atomic Energy Association. The channel number and the characteristic energy are related by polynomial equation 4.1.

$$y(x) = kx^2 + nx + m \ldots\ldots\ldots\ldots\ldots\ldots\ldots\ldots\ldots\ldots\ldots\ldots\ldots\ldots\ldots\ldots 4.1.$$

A multi-nuclide reference standard material supplied by IAEA which contained Americium-241, Caesium-137 and Cobalt-60 was used for the calibration (IAEA, 1987).The channel numbers and corresponding energies are as shown in table 4.1

Table 4.1: Detector Energy Calibration

RADIONUCLIDE	CHANNEL	ENERGY (KEV)
Am-241	34.1	60.0
Cs-137	329.6	663.35
Co-60	565.5	1172.69
Co-60	637.3	1332.69

The standard reference materials spectrum gave data that was used for energy channel fitting as shown in figure 4.3.

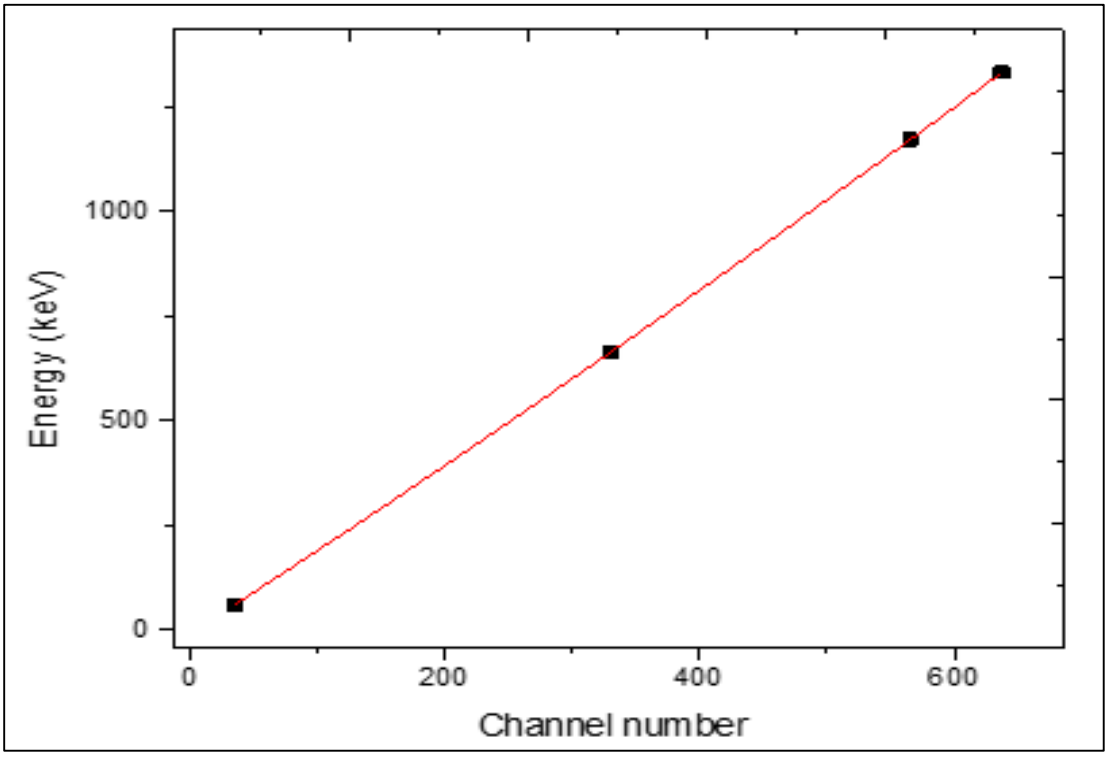

Figure 4.3: Energy Calibration Fitting used in this Study

The line represents a second-order polynomial fit which is defined by equation 4.2.

$$y = 0.0002x^2 + 1.9612x7.1308 \ldots\ldots\ldots\ldots\ldots\ldots\ldots\ldots\ldots\ldots\ldots\ldots\ldots\ldots\ldots\ldots \quad 4.2.$$

Fitting of the energy points assisted in identifying the energies of the unknown peaks in the spectrum.

4.5.2 Energy Resolution

Energy resolution measures how good a detector can differentiate between two peaks with close energies in a spectrum. This feature depends on full width at half maximum value of the generated pulse. At 662KeV energy, the sodium iodide counter has a resolution of about 7% which is low(Wang, 2003). The poor resolution makes this detector inefficient when dealing with samples composing multiple isotopes. The energy resolution in this study was determined using equation 4.3 and the obtained energies are shown in table 4.2.

$$R = \frac{FWHM}{Ec} \ldots\ldots\ldots\ldots\ldots\ldots\ldots\ldots\ldots\ldots\ldots\ldots\ldots\ldots\ldots\ldots\ldots\ldots 4.3$$

Whereby, R is the energy resolution while E_c is the centroid energy.

Table 4.2: Detector Energy Resolution

Radionuclide	Energy(Kev)	FWHM	Resolution
Cs-137	663.35	43.78	6.6%
Co-60	1172.69	55.59	4.7%
Co-60	1332.69	60.09	4.5%

Figure 4.4 is a graph of the detector resolution against the energies obtained.

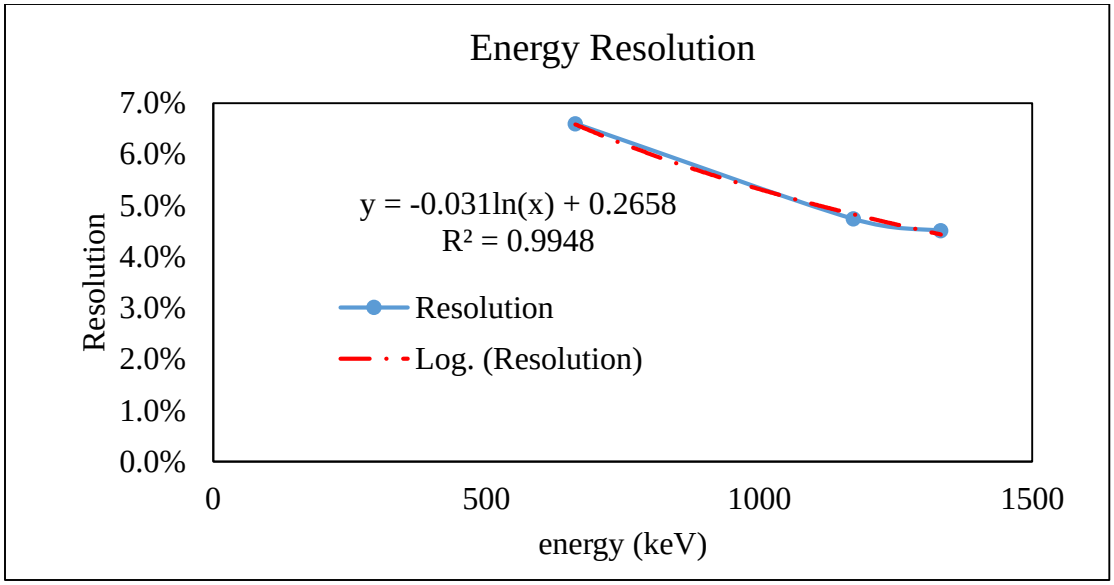

Figure 4.4: Detector Energy Resolution Graph.

Although it has a low resolution, the thallium activated sodium iodide detector has many desirable characteristics including its availability in large sizes at moderate cost, its good optical quality, its linear dependence of the amount of light generated on deposited energy, and also high scintillation efficiency.(Kelleter *et al.*, 2020).

4.5.3 Detector Counting Efficiency

It is the ratio of the detector counts registered to the total number of radiations emitted by the source. It is dependent on the type of incident radiation and its energy as well as the distance of separation between the detector crystal and the sample. Sodium iodide detector is a scintillation counter with a very short dead time.

In this study the average dead time was 0.01%. The detector crystal and the sample were in contact which guarantees efficiency. For this work, the efficiency for the standard radio nuclides was obtained using equation 4.4.

$$\eta = \frac{N}{AM\varrho T} \dots\dots\dots\dots\dots\dots\dots\dots\dots\dots\dots\dots\dots\dots\dots\dots\dots\dots\dots\dots\dots\dots.4.4$$

Whereby, N is the net counts, A is the standard sample's activity concentration, M is the mass of the standard sample in kilograms, ϱ is the gamma rayemission probability of the radionuclide and T is the live time in seconds. Table 4.3 shows the efficiency and intensities for the standard radio nuclides used.

Table 4.3: Intensity and Efficiency, for the Standard Radio Nuclides used.

Nuclide	**Energy (KeV)**	**Intensity**	**Emission Probability**	**Activity**	**Mass(Kg)**	**Efficiency(η)**
Th-232	238	26.46661	0.4316	3250	0.236	0.079951
U-238	351	19.5907	0.3534	4940	0.239	0.046952
K-40	1460	8.757	0.1066	14000	0.279	0.021031

4.5.4 Measurement of the Background Radiation

Background radiation is the omnipresent natural radiation in the environment that is not resulting from a test sample. It is the reason why a detector registers some counts in the absence of a test sample. This background count may result from terrestrial radio nuclides like ^{232}Th, ^{238}U and ^{40}K in the environment of the detector, cosmic radiation from the atmosphere and also radio nuclides like ^{137}Cs and ^{90}Sr artificially present within the environment depending on the level of technology and the population distribution of a given region (Matsitsi2020). Before the measurement of the samples was done, the background contributions were measured by running deionized water in a similar container as those containing the samples for 28800 seconds. Deionized water was preferred to any other water for it is inert and nonradioactive. Filling the container with water also was done to drive out all air inside reducing chances of radioactive radon gas in the container.

Figure 4.5 shows the background spectrum developed by running deionized water

in a container the same dimensions as those used for the samples.

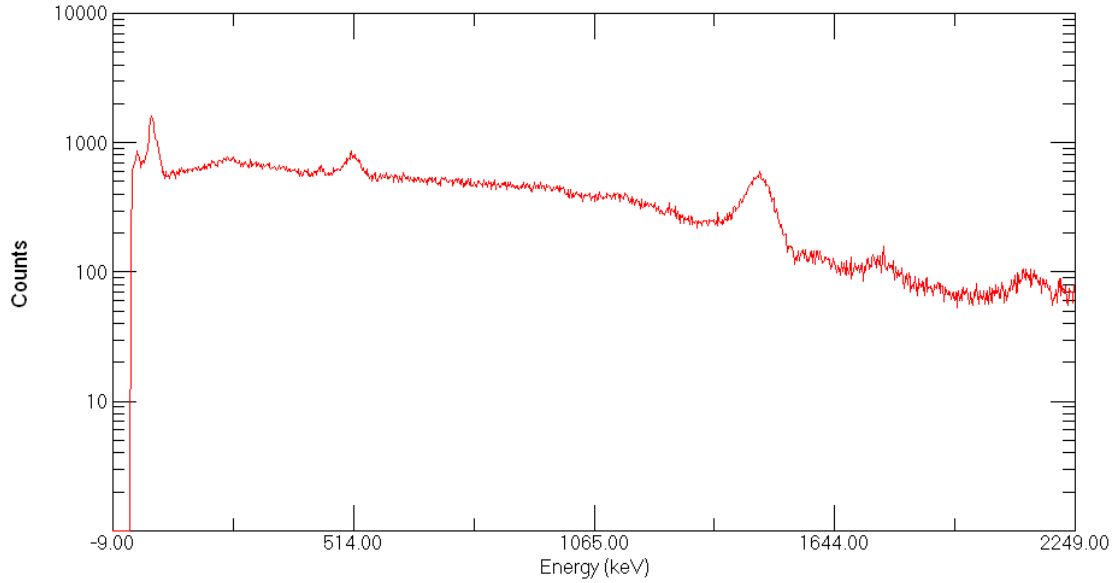

Figure 4.5: Background Spectrum using Deionized Water.

The peaks in the spectrum confirmed presence of background radiation in the environment and therefore its count was taken and subtracted from the gross count, to get the net count rate resulting from the radio nuclides in the tile samples.

4.5.5 Data Acquisition

To measure the activity, each tile sample was separately lodged into the shielded NaI (Tl) detector and ran for 28800 seconds. Spectra for all the samples were acquired and stored ready for recall to generate the region of interest, gross area count, centroid channel and energy of the corresponding radio nuclides. Ortec maestro software was installed in a computer to perform the analysis of each gamma-ray spectrum produced. The number of counts as seen from any region of interest corresponded to the abundance of the radioactive material in the measured sample while the measured energy corresponds to the type of the element and its isotope. The information obtained was presented in tables, charts, and graphs for ease of interpretation.

4.6 Evaluation of Radiometric Parameters

4.6.1 Specific Activity Concentration of Radio Nuclides in $BqKg^{-1}$

For Uranium (^{238}U) the Specific activity concentration in this work was determined from the counts of lead (^{214}Pb), similarly, for thorium (^{232}Th), it was determined from the counts of ^{212}Pb and finally, the activity of potassium (^{40}K) was determined from the counts of 1460.83 Kev. Equation (4.5) was used to determine the specific radionuclide activity given in $BqKg^{-1}$ (Ebaid, 2010).

$$A_c = \frac{N_p}{p.\eta.m} \ldots\ldots\ldots\ldots\ldots\ldots\ldots\ldots\ldots\ldots\ldots\ldots\ldots\ldots\ldots\ldots\ldots\ldots\ldots\ldots\ldots\ldots\ldots\ldots\ldots\ldots\ldots\ldots 4.5$$

Where, N_p is the net count rate (cps), that is (gross minus background value), p is the gamma-ray yield or emission probability, η (E) is the absolute counting efficiency of the detector while m is the sample mass in (kg).

4.6.2 Radium Equivalent Activity (Ra_{eq})

This refers to the weighted sum of the activities of ^{226}Ra, ^{232}Th, and ^{40}K assuming that $1BqKg^{-1}$ of ^{226}Ra, $0.7BqKg^{-1}$ of ^{232}Th and $13BqKg^{-1}$ of ^{40}K produce the same gamma radiation dose rate (Beretka& Matthew, 1985). The equation 4.6 is the relation used to calculate this radium equivalent.

$$Ra_{eq} = C_{Ra} + 1.423C_{Th} + 0.077C_K \ldots\ldots\ldots\ldots\ldots\ldots\ldots\ldots\ldots\ldots\ldots\ldots\ldots\ldots\ldots\ldots 4.6$$

Whereby, Ra_{eq} is the radium equivalent, while C_{Ra}, $C_{Th,}$ and $C_k$are the activity concentrations of ^{226}Ra, ^{232}Th and ^{40}K in tile powder samples respectively given in $BqKg^{-1}$. For safety, any building material with $Ra_{eq}>370BqKg^{-1}$ should not be used as it poses a high radiation exposure hazard (UNSCEAR, 1988).

4.6.3 Estimation of the Absorbed Dose Rate (D)

Absorbed dose is an expression of the concentration of radiation energy that is absorbed at a specific point in the body tissue. These absorbed gamma radiation dose rates were calculated from the corresponding activity concentration of ^{226}Ra, ^{232}Th and ^{40}K using the activity concentration-dose ($nGyh^{-1}$ per $BqKg^{-1}$) conversion factors of 0.427, 0.662 and 0.043 provided by UNSCEAR (2000). Equation 4.7 shows how to calculate the dose rate.

$$D = 0.427CRa + 0.662CTh + 0.043CK + 0.043C \ldots\ldots\ldots\ldots 4.7$$

Where, C_U, C_{Th} and C_K are the average activity concentration of Uranium-238, Thorium-232 and Potassium-40 respectively.

4.6.4 Annual Effective Dose Rate (AED)

The annual effective dose rate received by a given population and which is attributed to radioactivity is estimated using a conversion factor of $0.7SvGy^{-1}$. For adults about 60% of their time is spent indoors, while 40% is time outdoors(Mustapha, 1999). This gives an indoor occupancy factor of 0.6 and 0.4 outdoor occupancy factor (UNSCEAR, 2000). The indoor and outdoor annual effective doses rates were therefore calculated by the given equations 4.8 and 4.9 respectively.

$$E_{in} = D\ x8760hy^{-1}x\ 0.6\ x\ 0.7SvGy^{-1}\ x\ 10^{-6} \ldots\ldots\ldots\ldots\ldots\ldots\ldots\ldots\ldots\ldots 4.8$$

$$E_{out} = D\ x\ 8760hy^{-1}\ x\ 0.4\ x\ 0.7SvGy^{-1}\ x\ 10^{-6} \ldots\ldots\ldots\ldots\ldots\ldots\ldots\ldots\ldots 4.9$$

Whereby E_{in} and E_{out} are the Annual Effective Doses rates for indoor and outdoor environments respectively, $D(nGyh^{-1})$ is the absorbed dose in air, $8760hy^{-1}$ is the number of hours in one year, $0.7(SvGy^{-1})$ converts the absorbed dose in the air to annual effective dose and 0.4 is the outdoor occupancy factor (UNSCEAR, 2017)

4.6.5 External Hazard Index (H_{ex})

This is the measure of gamma radiation exposure to humans externally. This exposure may occur when the body encounters elevated energy radiation from the ceramic tiles. For a given radiation to have insignificant hazardous effects to humans, its value of the external hazard index has to be less than 1 (Tsai *et al.*, 2008). The external Hazard index was determined using the equation 4.10.

$$H_{EX} = \frac{C_{Ra}}{370} + \frac{C_{Th}}{259} + \frac{C_K}{4810} \ldots\ldots\ldots\ldots\ldots\ldots\ldots\ldots\ldots\ldots\ldots\ldots\ldots\ldots 4.10$$

Where, C_{Ra}, C_{Th} and C_K are the average activity concentrations of the three primordial radio nuclides expressed in $BqKg^{-1}$.

4.6.6 Internal Hazard Index (H_{in})

Internal radiation exposure to a human being may result from inhaling terrestrial radio nuclides like ^{40}K, ^{238}U and ^{232}Th and their progenies in air around the vicinity of the tiles.

The internal hazard index (H_{in}) was calculated using equation 4.11.as formulated by(Beretka & Mathew, 1985)

$$H_{in} = \frac{C_{Ra}}{185} + \frac{C_{Th}}{259} + \frac{C_K}{4810} \ldots\ldots\ldots\ldots\ldots\ldots\ldots\ldots\ldots\ldots\ldots\ldots\ldots\ldots 4.11$$

Where, C_{Ra}, C_{Th}, and C_K are the mean activity concentrations in $BqKg^{-1}$ of ^{226}Ra, ^{232}Th and ^{40}K respectively. The value of this index also has to be below a unit for the radiation to be termed safe to humans.

CHAPTER FIVE

5.0 RESULTS AND DISCUSSIONS

5.1 Introduction

Gamma ray spectrometric analysis for representative ceramic tiles samples in the Kenyan market has been studied. The identity, quantity, and the energy content of the radio nuclides present in the tiles have been established. The radiological parameters like radium equivalent, absorbed dose rate, annual effective dose and hazard indices obtained have been compared with previous studies and the respective world's recommended thresholds to establish their potential harm to human beings. These results are presented in the following sections and sub sections.

5.2 Results

A total of 37 samples were prepared, tested and analyzed following procedures and methods discussed in chapter four. A spectrum obtained for each of the sample, gross count rate and energy peaks for each radionuclide was determined. These were used to evaluate the activity concentration of the radio nuclides ^{238}U, ^{232}Th and ^{40}K for the samples. Figure 5.1 is a typical sample spectrum obtained during data acquisition.

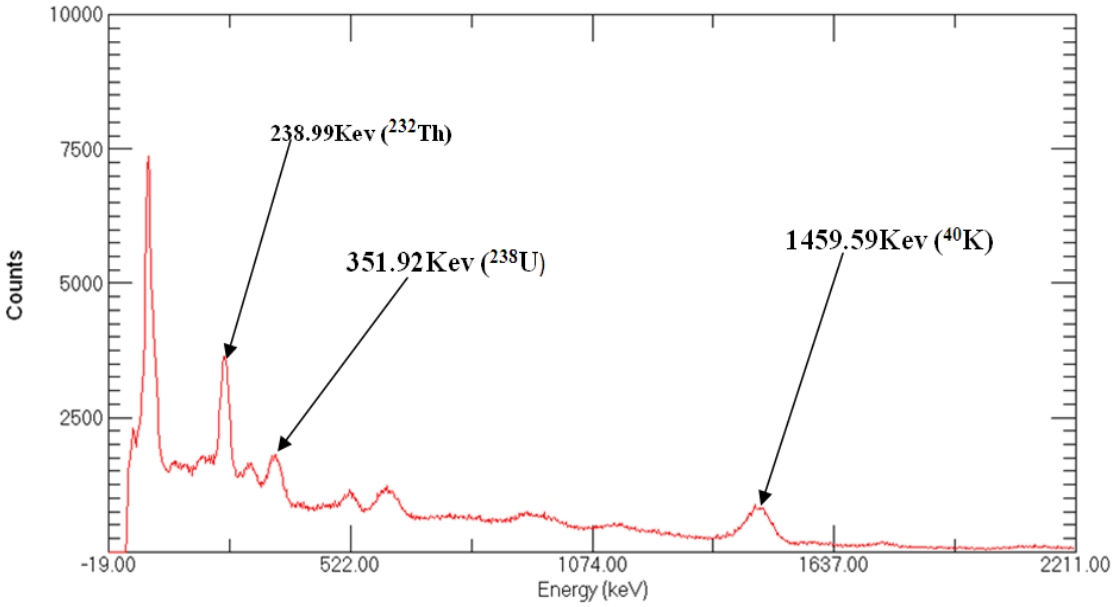

Figure 5.1: A Spectrum of one of the Tile Samples (CV001W).

The spectrum shows peaks for some primordial radio nuclides and their corresponding energies. The hypothesis that ceramic building tiles contain radio nuclides ^{232}Th, ^{238}U and ^{40}K was therefore confirmed. Other radiological parameters like; radium equivalent activity, hazard indices and dose rates have been calculated from activity concentration using conversion factors specified in sub sections 4.6.Each of these parameters will be discussed independently in subsections 5.2.1 to 5.2.5.

5.2.1 Activity Concentrations of Natural Radio Nuclides.

In this study the activity concentration of primordial radio nuclides^{232}Th, ^{238}U and ^{40}K was determined using equation 4.5. Table 5.1 gives the activity concentration of the three primordial radio nuclides (^{232}Th, ^{238}U and ^{40}K) in the 37 samples.

Table 5.1: Activity Concentration of the Three Radio Nuclides (^{232}Th, ^{238}U and ^{40}K)

S/N	Sample code	Activity concentration in $BqKg^{-1}$					
		^{232}Th	Error (±)	^{238}U	Error (±)	^{40}K	Error (±)
1	CVOO1W	116.21	3.23	60.8	6.52	667.18	49.59
2	CV002W	93.53	3.07	39.93	5.91	623.95	47.27
3	CV003W	112.42	2.98	60.34	5.77	727.12	45.73
4	CB001W	101.96	2.66	71.23	3.2	124.5	28.83
5	CB002W	63.07	1.54	45.42	2.61	415.92	31.14
6	IX001W	98.06	3.10	30.39	2.24	61.25	31.22
7	IX002W	100.98	2.87	52.21	5.86	446.74	47.82
8	KS001W	45.97	2.28	48.21	4.74	880.58	45.32
9	KS002W	48.88	2.11	48.04	4.42	360.46	30.76
10	KSOO1F	48.52	2.77	4.01	1.42	810.47	36.66
11	KS002F	46.49	1.59	47.74	2.64	786.17	35.64
12	KS003F	51.31	1.80	40.56	2.63	506.29	31.44
13	KS004F	55.53	1.80	34.68	2.30	534.3	32.09
14	KS005F	63.03	1.67	39.5	3.23	1533.28	31.95
15	KSJ001W	50.28	2.12	83.42	3.31	634.52	31.81
16	KSJ002W	36.78	1.47	62.11	2.67	432.5	31.98
17	KT001W	29.75	1.36	36.69	2.63	308.8	30.09
18	KT002W	40.32	2.42	25.78	5.27	667.63	42.92
19	KT003W	37.52	1.51	37.21	2.57	345.41	31.82
20	KT004F	52.99	2.19	0.65	1.02	365.28	30.39
21	KT005W	37.52	1.51	37.21	2.57	367.75	31.82
22	KBL001F	52.65	2.60	37.14	5.04	1051.81	45.42
23	KBL002F	49.60	2.57	57.39	3.85	1013.41	44.46
24	UG001F	78.58	3.20	85.66	3.16	544.18	35.67
25	UG002F	77.31	3.28	76.02	3.61	332.84	32.54
26	UG003F	34.00	2.48	110.21	3.40	532.63	34.58
27	UG004F	34.12	4.38	124.79	4.04	272.09	32.09
28	UG005F	5.71	5.09	78.53	7.07	347.83	33.79
29	TG001W	28.73	1.39	18.81	2.24	753.97	27.35
30	TG002W	37.32	2.17	34.28	3.35	271.29	41.33
31	TG001F	47.01	2.37	6.09	6.06	867.68	43.22
32	TG002F	36.80	2.21	6.28	1.67	757.98	44.17
33	TG003F	38.92	2.20	12.18	1.88	757.61	44.14
34	TS001F	41.92	2.03	1.02	0.92	59.23	28.94
35	TS002F	23.10	1.2	14.07	2.25	121.43	31.85
36	TS003F	31.34	1.38	20.06	2.22	103.36	31.32
37	TS004F	39.66	2.00	8.70	1.64	74.04	28.6
MIN		5.71	1.20	0.65	0.92	59.23	27.35
MAX		116.21	5.09	124.79	7.07	1533.28	49.59
AVERAGE		53.73	2.34	43.17	3.40	525.99	36.10

Table 5.2 shows the mean activity concentration of the radio nuclides in this study compared with the world's averages.

Table 5.2: Mean Activity Concentration Versus World's Averages.

Radionuclide	Results of this study $BqKg^{-1}$	World's average in $BqKg^{-1}$
^{232}Th	53.73±2.34	45
^{238}U	43.17±3.40	33
^{40}K	525.99±36.10	420

As seen from table 5.2, the mean values obtained were 53.73 ±2.34$BqKg^{-1}$ for ^{232}Th, 43.17±3.40$BqKg^{-1}$ for ^{238}U and 525.99±36.10$BqKg^{-1}$ for ^{40}K. All these values exceeded the world's averages of 45$Bqkg^{-1}$, 33$BqKg^{-1}$ and 420$BqKg^{-1}$ for ^{232}Th, ^{238}U and ^{40}K respectively (UNSCEAR, 2017). The Maximum values observed were 116.21±5.09$BqKg^{-1}$ for ^{232}Th, 124.79±7.07$BqKg^{-1}$ for ^{238}U and 1533.28±49.59$BqKg^{-1}$ for ^{40}K.The minimum values from the study were 5.71±1.2$BqKg^{-1}$ for ^{232}Th, 0.65±0.92$BqKg^{-1}$ for ^{238}U and 59.23±27.35$BqKg^{-1}$ for ^{40}K.The activity concentrations emanating from ^{40}K, ^{238}U and ^{232}Th for this present study exceeded national average (Kenya) of 255.7$BqKg,^{-1}$ 28.7$BqKg^{-1}$ and73.3$BqKg^{-1}$ respectively(Otwoma *et al.,* 2012). However, the average activity levels of ^{232}Th, ^{238}U and ^{40}K are very close to the national averages and worldwide averages(Otwoma *et al.,* 2012).

The findings are well in range with the geological profile reported in literature by other scholars (Nyamai*et al.,* 2001),and Nalianya *et al*., 2022). The activities of^{232}Th, ^{238}U and ^{40}K have been presented graphically in the figure 5.2, 5.3 and 5.4 respectively. Figure 5.2, 5.3 and 5.4 is the graphical representation of the activity concentration of ^{232}Th ^{238}U and ^{40}K in the 37 samples. The red line represents the world's averages.

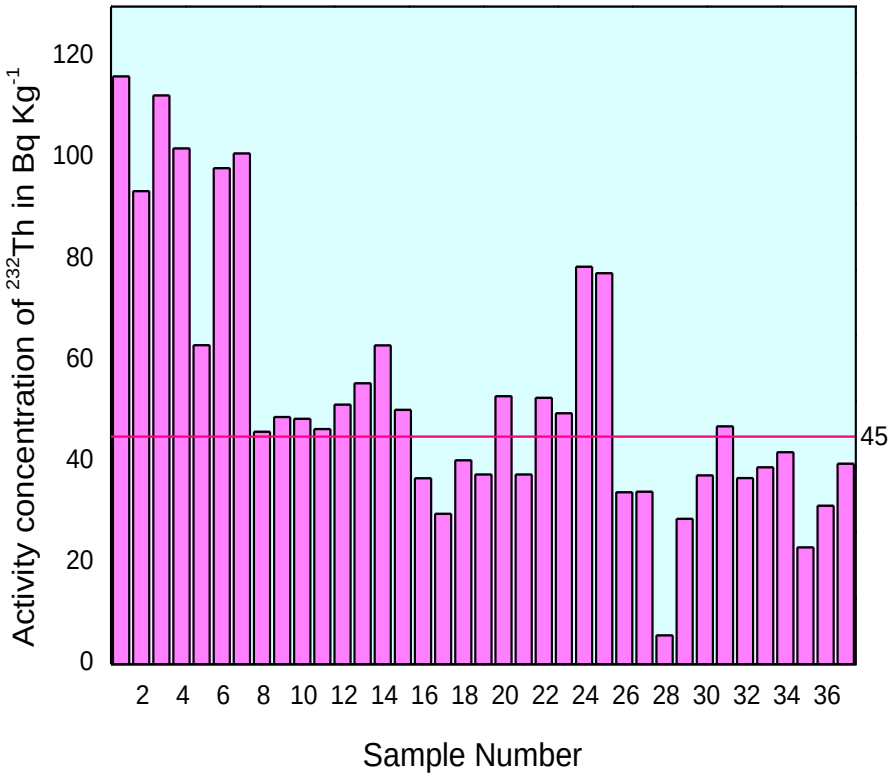

Figure 5.2: A Graph Showing the Activity Concentration of ^{232}Th in the 37 Tile Samples.

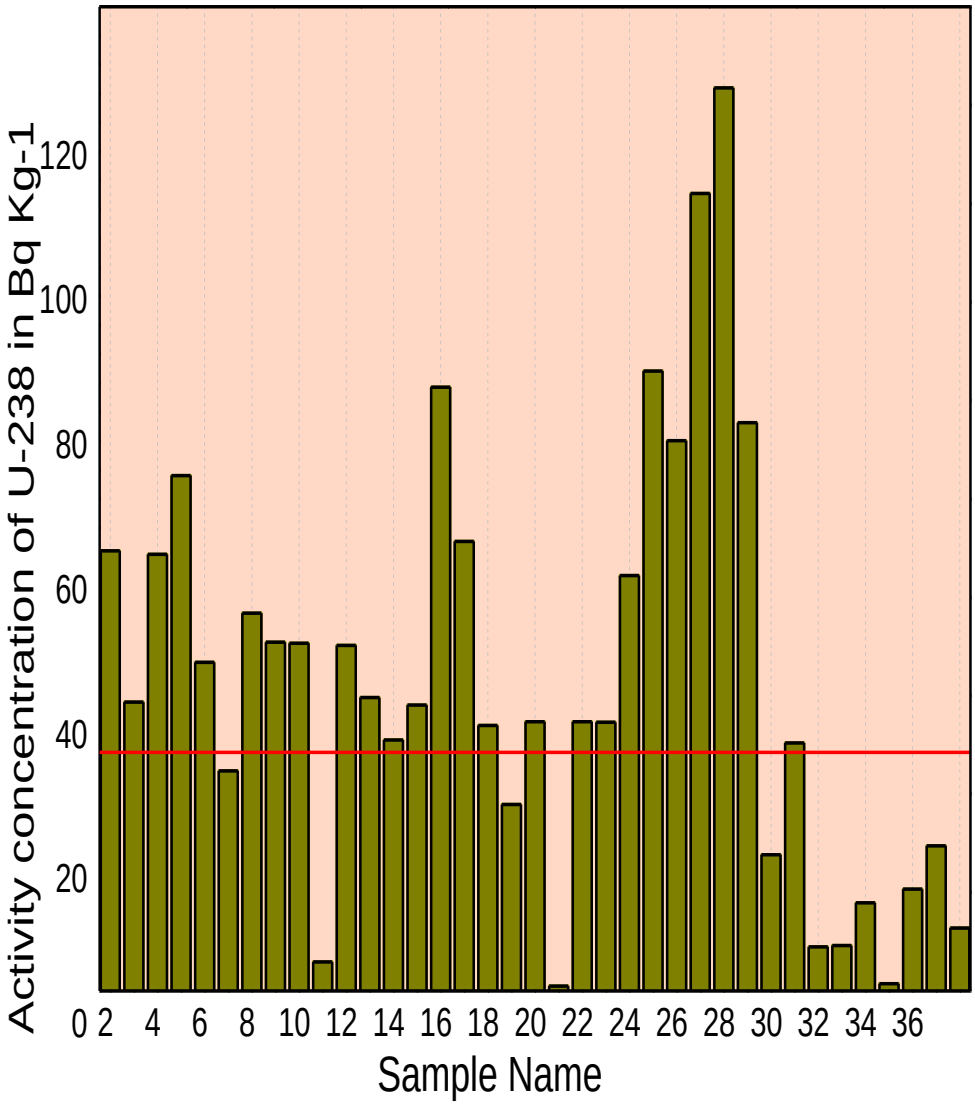

Figure 5.3: A graph Showing the Activity Concentration of ^{238}U in the 37 Samples.

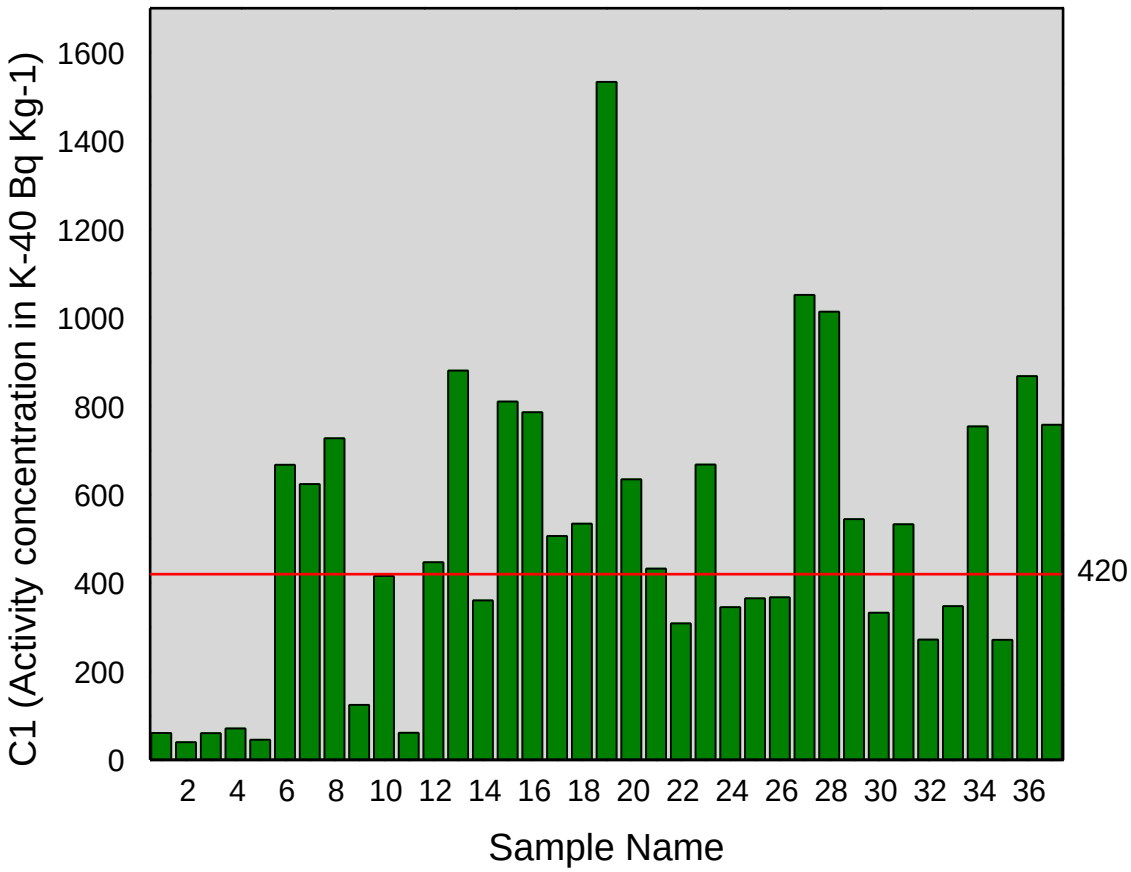

Figure 5.4: Activity Concentration of ^{40}K in the 37 Samples.

Generally, in each of the three figures more than half of the sampled tiles had elevated activity concentration values. This indicated considerable levels of the primordial radioisotopes, ^{232}Th, ^{238}U and ^{40}K, in the soils from which the tiles are manufactured. Studies show that Radioactivity of a given soil relates to the rock type from which the soil comes with igneous rocks giving higher radiations and sedimentary rocks lower values (UNSCEAR 2000). The values observed here are therefore characteristic of the meta-igneous rocks present in all regions within the Mozambique belt of which Kenya, Uganda, India and Tanzania are part.

In Kenya, (where 16 out of the 37 sampled tiles are manufactured) most ceramic tile companies are found in Kajiado, Mombasa and Nairobi counties. Kajiado County covers a region rich in crystalline lime stones, quartzite, gneisses granulites and potash soils which

contain high levels of natural radioactivity(Matheson, 1966). The highest registered activity concentration value of ^{40}K was 1533BqKg^{-1} posted by a Kenyan tile sample (KS005F). This is attributed to the high level of potassium in Kenyan soil especially in coastal regions.(Kebwaro *et al.,* 2011)reported elevated levels of background radiation from ^{232}Th, ^{238}U and ^{40}K in the south coast of Kenya which was attributed to abundance of minerals like carbonatites and monazites. Kenyanya*et al.,* (2013) investigated potassium content in Kenyan soil and found that 70% of the mapped sites confirmed potassium present.

Considering ^{232}Th and ^{238}U, tiles from Tanzania posted the lowest values for activity concentration. This agrees with a study done in Tanzania that listed the major soil types in the country as ferric, chromic and eutric cambisols which contain very little thorium and uranium (Msanya*et al.,* 2002).According to Graef *et al.*,(2015), potassium was found to be limited in surface soil and only presently abundant between 50 and 300 meters underground. This relates positively with the low activity concentration of the three radio nuclides in Tanzania tile samples.

The three radio nuclides were confirmed present in all the tiles sampled. This agrees with the (UNSCEAR 2000) report that natural radioactivity is present in the soils of all regions of the world. Samples from different countries analyzed in this study posted different averages for the activity concentrations as shown in table 5.3. This results from uneven distribution of the radio nuclides in different soils of the different regions.

Table 5.3 compares activity concentration of the three radio nuclides from this study and other studies across the world.

Table 5.3: Activity Concentration of ^{232}Th, ^{238}U and ^{40}K for this Study Compared with Other Studies.

	Country	**^{238}U(^{226}Ra)**	**^{232}Th**	**^{40}K**
This study	Tiles from Kenya	83.3	46	921
	Tiles from Tanzania	17.5	35	463
	Tiles from Uganda	100	41.5	816
	Tiles from China	55	61	426
	Tiles from India	41	99	253.5
Other studies	Kenya(Nalianya *et al*., 2022)	109	11	1574
	Sudan(Saif*et al*., 2022)	183	51	238
	Sudan(Adrean *et al.*,2020)	12-40	10-70	28-94
	Nigeria(Ademola *et al*., 2009)	72	84	629
	South Korea (Lee, 2005)	44-82	34-96	310-1019
	Algeria (Amrani, 2001)	55	41	410
	China (Xinwei, 2005)	64-131	55-107	561-867
	India (Mahur, 2008)	28	64	24
	Greece (Krstić, 2007)	25-174	29-47	411-786
	Egypt (Afifi, 2005)	61-118	55-98	730-1050
	Spain (Rami, 2007)	75-191	68-76	507-490
	Italy (Righi, 2009)	36-87	38-86	411-996
	Italy (Righi, 2009)	20-708	33-145	158-850
	Nigeria (Joel *et al.,* 2018)	61.1	70.2	514.7
	Saudi Arabia (Alghamdi, 2019)	29-129	32-114	83-1100

The findings from this work compares well with similar studies done in different parts of the world. The close comparison of activities for each element was attributed to similarities in raw materials (rock) used in tile production.

The activity concentrations of the three radio nuclides ^{232}Th, ^{238}U and ^{40}Kgiven in table 5.1 were used to estimate the measure of human exposure to gamma ray energy by calculating

the radium equivalent, the absorbed dose, annual effective doses as well as the hazard indices. These parameters were calculated using standard equations 4.6, 4.7, 4.8, 4.9 and 4.10.

Table 5.4 shows the radium equivalent activity and the absorbed dose rates for the 37 samples.

Table.5.4: Radium Equivalent Activity and the Absorbed Dose Rates for the 37 Samples.

S/N	Sample code	Radium equivalent($BqKg^{-1}$)	Absorbed dose rate($nGyh^{-1}$)
1	CVOO1W	277.53	131.11
2	CV002W	221.06	105.79
3	CV003W	276.31	103.32
4	CB001W	225.91	103.27
5	CB002W	167.19	79.03
6	IX001W	174.65	80.53
7	IX002W	230.31	108.35
8	KS001W	181.42	88.88
9	KS002W	145.35	68.37
10	KSOO1F	135.46	68.68
11	KS002F	174.43	84.97
12	KS003F	152.56	73.06
13	KS004F	154.84	74.54
14	KS005F	247.26	124.52
15	KSJ001W	203.83	96.19
16	KSJ002W	147.76	69.47
17	KT001W	102.8	48.64
18	KT002W	134.56	55.4
19	KT003W	117.2	55.58
20	KT004F	104.18	51.07
21	KT005W	118.92	56.54
22	KBL001F	193.04	95.94
23	KBL002F	206	100.92
24	UG001F	219.72	111.99
25	UG002F	211.66	97.95
26	UG003F	199.61	92.47
27	UG004F	194.29	87.57
28	UG005F	113.44	52.27
29	TG001W	117.75	59.47
30	TG002W	108.27	51.01
31	TG001F	139.8	71.03
32	TG002F	117.02	59.64
33	TG003F	125.9	63.55
34	TS001F	65.22	30.73
35	TS002F	56.29	26.52
36	TS003F	72.61	33.76
37	TS004F	70.84	33.15
MIN		**56.29**	**26.52**
MAX		**277.53**	**131.11**
AV		**159.59**	**75.55**

5.2.2 Radium Equivalent

The activity concentration of a radionuclide equivalent to 370BqKg^{-1} of ^{226}Ra that gives exactly an external effective dose rate of 1.5mGy(1mSvy^{-1}) is the radium equivalent. Any building material with radium equivalent more than 370BqKg^{-1} is considered radio logically hazardous and therefore should not be used. A graph of the radium equivalent for all the 37 samples is as shown in figure 5.5

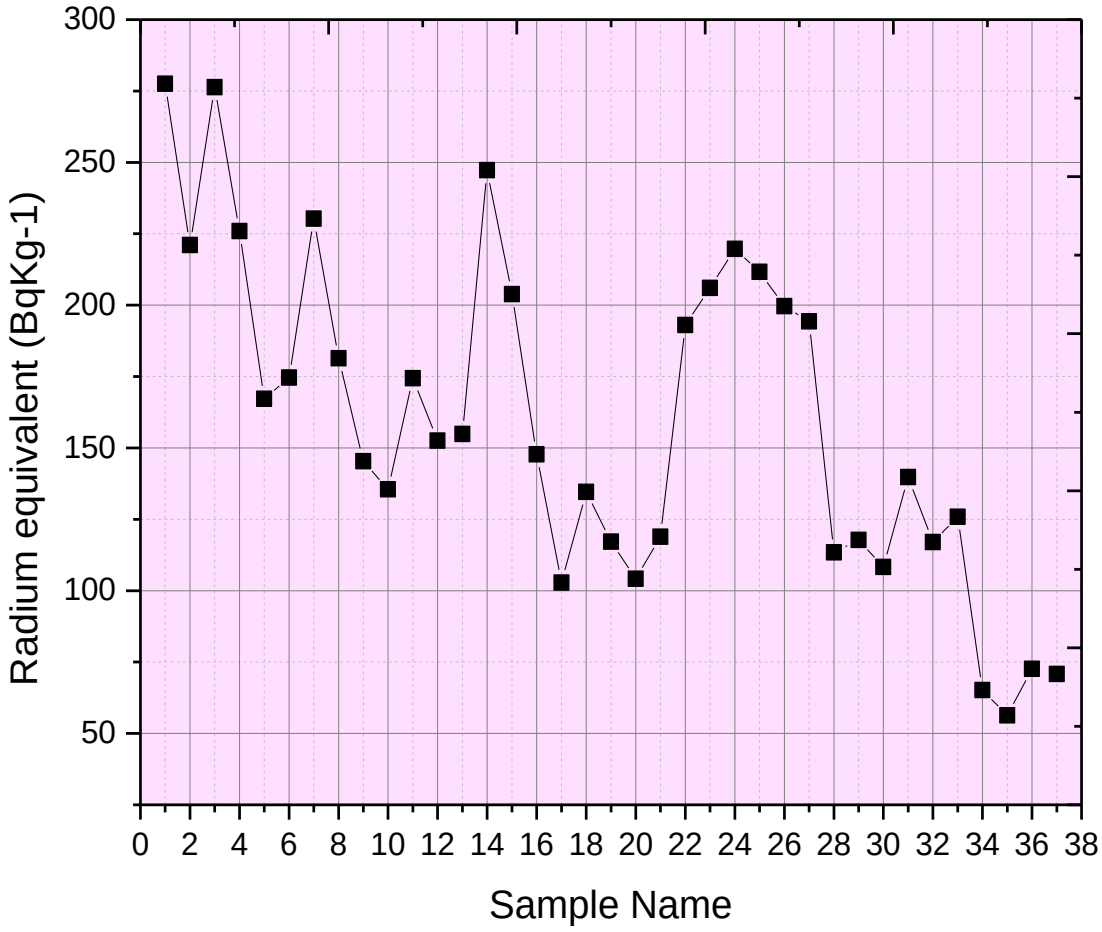

Figure 5.5: A Graph of the Radium Equivalent for all the 37 Tile Samples.

The average value of radium equivalent in this study was found to be 159.59 BqKg^{-1} which was above the world's average of 89BqKg^{-1} and lower than the safety limit of 370BqKg^{-1} (UNSCEAR 1988). The highest value of radium equivalent (277.53Bq Kg^{-1}) was for a sample (CV001W) followed by sample CV003W with 276.31BqKg^{-1}. Tiles from Tanzania posted radium equivalent values generally lower than all the other countries with the lowest

value being 56.29BqKg^{-1} for floor tile sample (TS002F). This observation was attributed to lower enrichments of ^{238}U, ^{232}Th and ^{40}K in the rock ore used during production. Non homogeneous distribution of radio nuclides in the environmental mediums could have led to the lower radium in this sample.

5.2.3 Absorbed Dose

Absorbed dose is the quantity of radiation energy absorbed by a unit mass of tissue. It is also the chemical or physical effect brought about by a given radiation exposure to bio matter. Figure 5.6 shows the values of absorbed dose for all the samples.

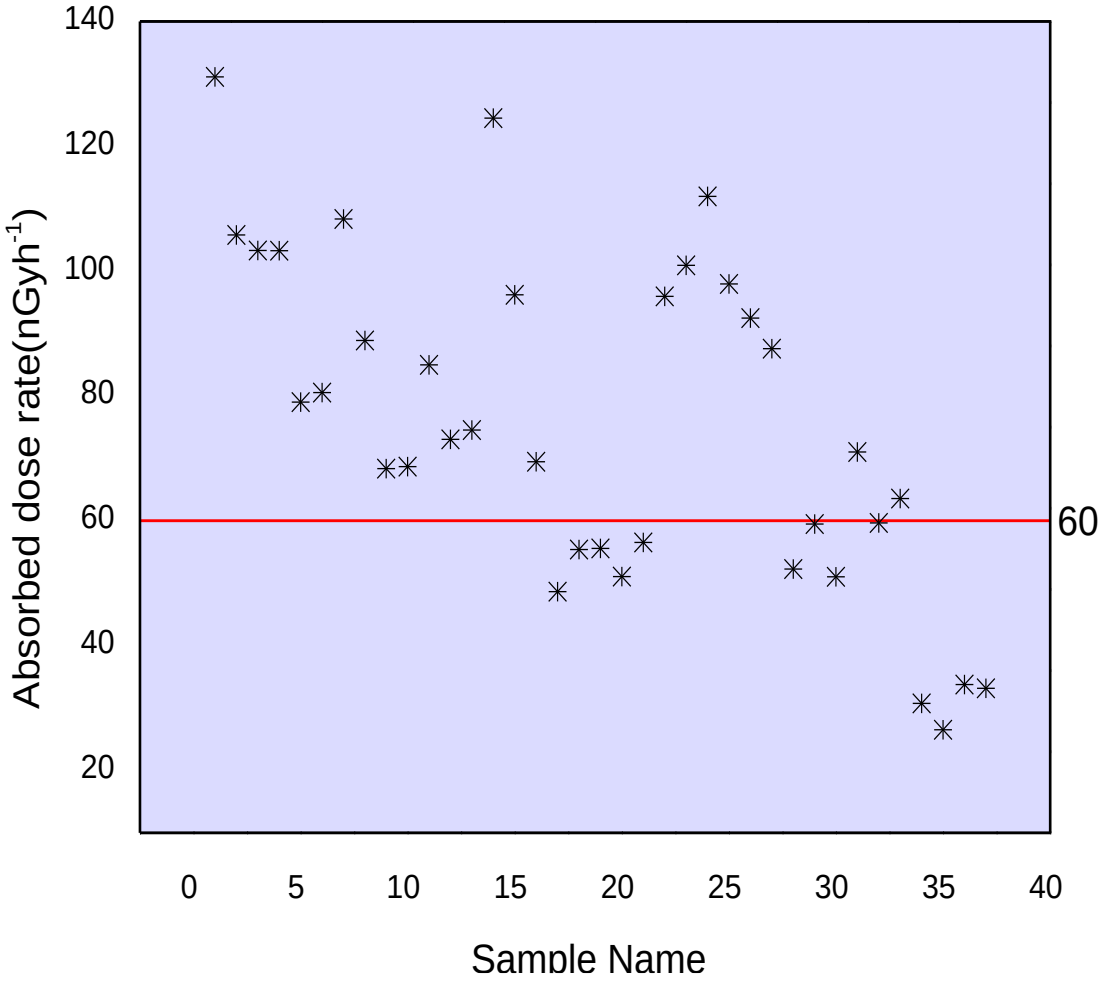

Figure 5.6: Absorbed Dose for the 37 Samples of Tiles used in Kenya.

The mean value of absorbed dose posted by this study was found to be 75.55nGyh^{-1} which was well above the world's average level of 60nGyh^{-1} but lower that the permissible safety

limit of 1500nGyh^{-1} as proposed by UNESCEAR 2016. The highest value of absorbed dose was 131.11nGyh^{-1} for sample CV001W while the lowest was 26.52nGyh^{-1} for sample TS002F.

The annual effective dose rates and hazard indices data from this study is given in table 5.5.

Table 5.5: The Annual Effective Dose and Hazard Indices.

S/N	Sample code	AED $_{in}$($mSvy^{-1}$)	AED $_{out}$($mSvy^{-1}$)	H_{ex}	H_{in}
1	CVOO1W	0.48	0.32	0.75	0.92
2	CV002W	0.39	0.26	0.6	0.71
3	CV003W	0.38	0.25	0.75	0.91
4	CB001W	0.38	0.25	0.61	0.8
5	CB002W	0.29	0.19	0.45	0.5
6	IX001W	0.3	0.2	0.47	0.56
7	IX002W	0.4	0.27	0.62	0.76
8	KS001W	0.33	0.22	0.49	0.62
9	KS002W	0.25	0.17	0.39	0.52
10	KSOO1F	0.25	0.17	0.37	0.38
11	KS002F	0.31	0.21	0.47	0.6
12	KS003F	0.27	0.18	0.41	0.52
13	KS004F	0.27	0.18	0.42	0.51
14	KS005F	0.46	0.31	0.67	0.78
15	KSJ001W	0.35	0.24	0.55	0.78
16	KSJ002W	0.26	0.17	0.4	0.49
17	KT001W	0.19	0.12	0.28	0.38
18	KT002W	0.2	0.14	0.36	0.43
19	KT003W	0.2	0.14	0.32	0.42
20	KT004F	0.19	0.13	0.28	0.28
21	KT005W	0.21	0.14	0.25	0.42
22	KBL001F	0.35	0.24	0.52	0.62
23	KBL002F	0.37	0.25	0.56	0.71
24	UG001F	0.41	0.27	0.65	0.88
25	UG002F	0.36	0.24	0.57	0.78
26	UG003F	0.34	0.23	0.54	0.84
27	UG004F	0.32	0.22	0.53	0.86
28	UG005F	0.19	0.13	0.31	0.52
29	TG001W	0.22	0.15	0.32	0.37
30	TG002W	0.19	0.13	0.29	0.39
31	TG001F	0.26	0.17	0.38	0.39
32	TG002F	0.22	0.15	0.32	0.33
33	TG003F	0.23	0.16	0.34	0.37
34	TS001F	0.11	0.08	0.18	0.18
35	TS002F	0.10	0.06	0.15	0.16
36	TS003F	0.12	0.08	0.20	0.25
37	TS004F	0.12	0.08	0.19	0.22
MIN		**0.10**	**0.06**	**0.15**	**0.16**
MAX		**0.48**	**0.32**	**0.75**	**0.92**
AVERAGE		**0.28**	**0.19**	**0.43**	**0.54**

5.2.4 Annual Effective Dose

Annual effective dose (AED) is the measure of radiation energy received by an individual in a year. It is measured indoor and outdoor for human beings who spend 60% of their time indoor and 40% outdoor (Mustapha 1999). If the Value exceeds a unit for any material, then that material is not safe for human handling (ICRP, 1990).Figure5.7 is shows the annual effective dose indoor for the samples.

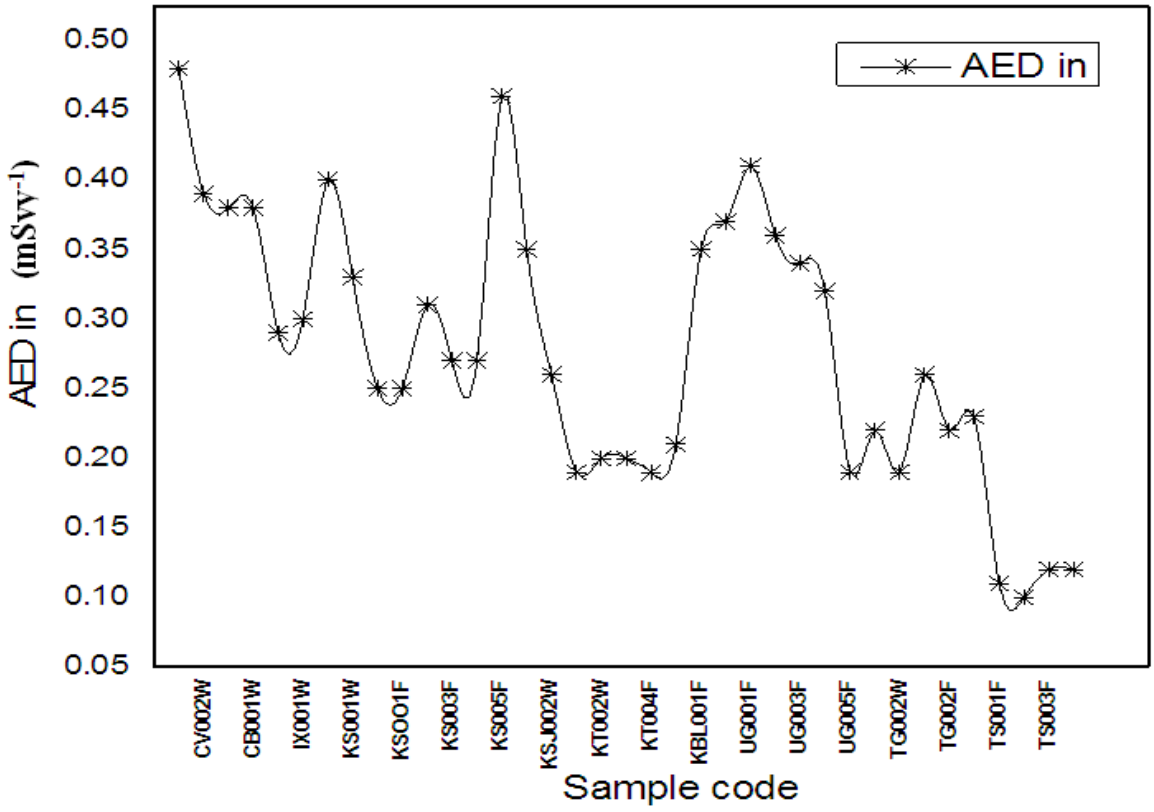

Figure 5.7: Annual Effective Dose Rate Indoor (Ein) for Tiles used in Kenya.

The mean value for indoor annual effective dose from this study was 0.28mSvy^{-1}.The overall highest value was 0.48mSvy^{-1} for sample CV001W which is a walling tile, while the lowest was 0.10mSvy^{-1} for sample TS002F a floor tile. The indoor values were found to be higher than outdoor values. This was attributed to the higher indoor occupancy factors. The indoor AED values were below the safety recommendation by UNSCEAR and ICRP reports of 1 mSvy^{-1}.

Figure 5.8 is the plot of the annual effective dose rate outdoor for the samples used in this study.

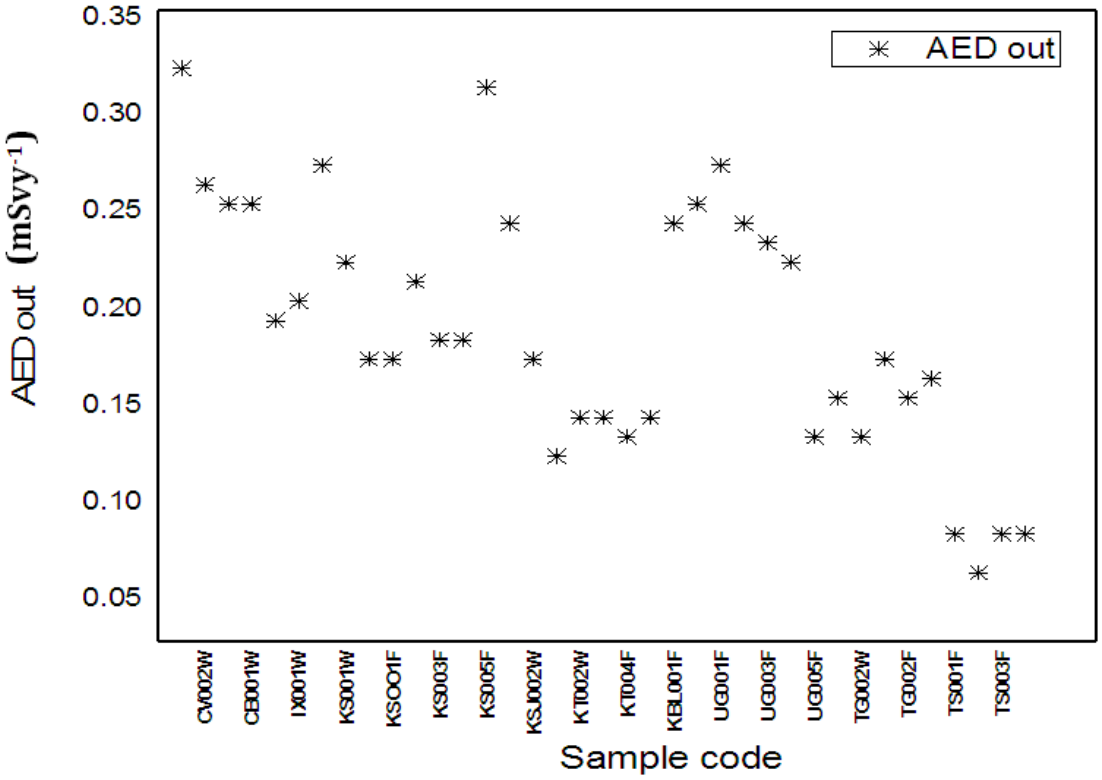

Figure 5.8: Annual Effective Dose Rate Outdoor (Eout) for Tiles used in Kenya.

The average value for outdoor annual effective dose from this study was 0.19mSvy^{-1}. The lowest registered value was 0.06mSvy^{-1} for TS002F while the highest was 0.32mSvy^{-1} for CV001W.Lower outdoor occupancy factor led to the outdoor values being generally lower than the indoor values.

5.2.5 Hazard Indices.

Internal hazard index is the measure of radiation exposure to an individual from radioactive substances within the body while external hazard index is the measure of the radiation exposure to an individual from radioactive substances outside the body. A material is radio logically unsafe if its hazard index exceeds 1.00 (ICRP, 2005).

Figures 5.9 and 5.10 gives the hazard indices values for the 37 samples.

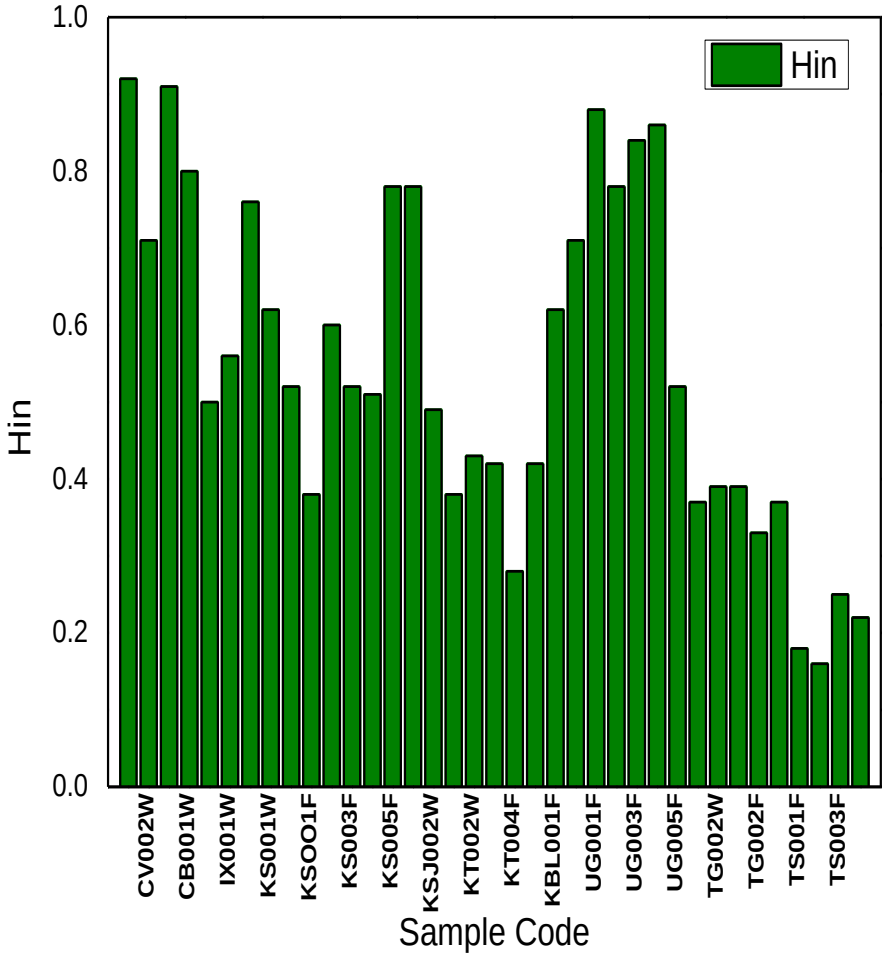

Figure 5.9: Internal Hazard Indices for the 37 Tile Samples

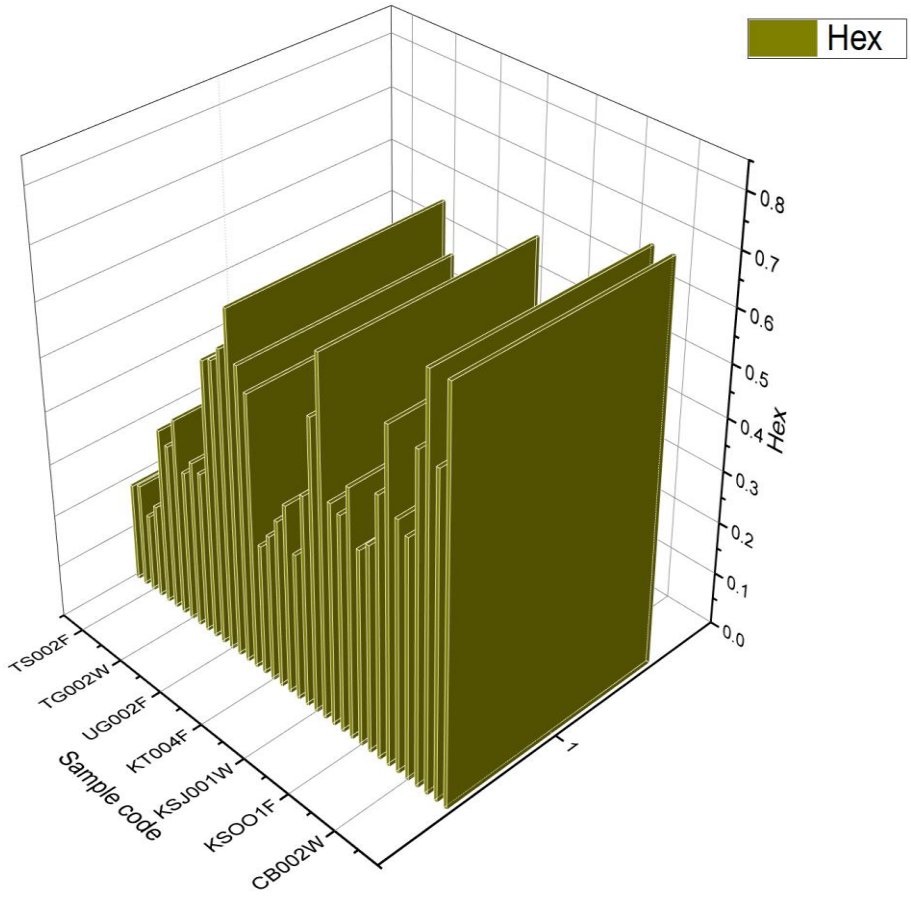

Figure 5.10: External Hazard Indices for the 37 Tile Samples

All the samples used in this study gave indices lower than a unit and therefore poses no health risk to human beings. The highest value of the internal hazard index was 0.92 for sample CV001W while the lowest was 0.16 for sample TS001F. The largest value of the external hazard index was 0.75 and the lowest was 0.15. The radiological parameters from this study were then compared with the world's recommended values as shown in table 5.6.

Table 5.6: Radiological Parameters of this Study Compared with World's Averages.

Parameter		**Si Unit**	**Recommended Value**	**Present Work (Average)**
Absorbed dose rate		Gyh^{-1}	60	75
Radium equivalent		$BqKg^{-1}$	370	159
Hazard indices	H_{in}	_	1	0.54
	H_{ex}	_	1	0.43
Annual Effective Dose	AED_{in}	$mSvy^{-1}$	1	0.28
	AED_{out}	$mSvy^{-1}$	1	0.19

The mean values for all the radiological parameters from this study were below the world's thresholds recommended by ICRP and UNSCEAR. This implies that the tiles in the Kenyan market as at the time of the study were safe for human handling.

CHAPTER SIX

6.0 CONCLUSIONS AND RECOMMENDATIONS

6.1 Conclusion

Measurement of the natural radioactivity of ceramic tiles used in Kenya has been well done using a shielded thallium doped sodium iodide detector. A total of 37 tile samples from different countries were analyzed to determine the radiation levels and radiological parameters evaluated. The research confirmed presence of radio nuclides ^{232}Th, ^{238}U and ^{40}K and their progenies in the building tiles used in Kenya. The analysis reported a mean activity concentration of 53.73 ±2.34$BqKg^{-1}$ for ^{232}Th, 43.17±3.40$BqKg^{-1}$ for ^{238}U and 525.99±36.10$BqKg^{-1}$ for ^{40}K. All this was found to exceed the world's averages of 45.00$BqKg^{-1}$, 33.00$BqKg^{-1}$ and 420.00$BqKg^{-1}$respectively. This was attributed to geology of the area from where the tiles raw materials comes, with igneous rocks giving higher radiations and sedimentary rocks lower values (UNSCEAR 2000). The values observed here are therefore characteristic of the meta-igneous rocks present in all regions within the Mozambique belt of which Kenya, Uganda, India, and Tanzania are part.

The activity concentrations values obtained for the three radio nuclides were used to calculate other radiological parameters like radium equivalent, absorbed dose, and annual effective dose (indoor and outdoor) and hazard indices (internal and external). The values were found to be 159.59$Bqkg^{-1}$, 75.55$nGyh^{-1}$, 0.28, 0.19, 0.54 and0.43respectively. All these radiological parameters were within the permissible thresholds as given in table 5.6, except the absorbed dose rate which was slightly higher. Based on the findings, the use of the ceramic tiles in Kenya for interior and exterior construction poses no harmful radiation exposure to the house dwellers. The parametric quantities which include annual effective dose, hazard indices and radium equivalent were below 1 $mSvy^{-1}$, a unit and 370$BqKg^{-1}$ respectively.

6.2 Recommendations

This study was conducted using ceramic tile samples from different manufacturers and countries. Based on the research findings, use of tiles for construction needs in Kenya poses

insignificant radiological risks to human health. From the study the following recommendations were made.

1. More radiometric studies are needed in this field since there is a continuous inflow of building tiles in the country. It is also expected that more companies from different countries are joining the industry as seen from the increasing demand for the tiles. This will help to determine decisively the health hazard involved.
2. Radiometric studies for other building materials like cement, quarry stones, sand and water should also be done for different areas of the country to ascertain the radiation levels in the soil.
3. To avert the effects of prolonged exposure to low doses of radiation, houses should have adequate ventilation to ensure quick escape of any radon gas which could emanate from the building materials used.

REFERENCES

Ademola, J. (2009). Natural radioactivity and hazard assessment of imported ceramic tiles in Nigeria. *African Journal of Biomedical Research, 12*(3), 161-165.

Adreani, T., Mattar, E., Alsafi, K., Sulieman, A., & Suliman, I. (2020). Natural radioactivity and radiological risk parameters in local and imported building materials used in Sudan. *Appl. Ecol. Environ. Res, 18*, 7563-7572.

Afifi, E. (2005). Characterization of the TE-NORM waste associated with oil and natural gas production in Abu Rudeis, Egypt. *Journal of environmental radioactivity, 82*(1), 7-19.

Alghamdi. (2019). Assessment of the chemical compositions and natural radioactivity in ceramic tiles used in some Saudi Arabian buildings. *Journal of the Australian Ceramic Society, 55*, 1099-1107.

Alghamdi, A. S., & Almugren, K. S. (2019). Assessment of the chemical compositions and natural radioactivity in ceramic tiles used in some Saudi Arabian buildings. *Journal of the Australian Ceramic Society, 55*, 1099-1107.

Ali, M. M., Zhao, H., Li, Z., & Maglas, N. N. (2019). Concentrations of TENORMs in the petroleum industry and their environmental and health effects. *Rsc Advances, 9*(67), 39201-39229.

Amana, M. S. (2017). Radiation hazard index of common imported ceramic using for building materials in Iraq. *Aust. J. Basic. Appl. Sci, 11*(10), 94-102.

Amrani. (2001). Natural radioactivity in Algerian building materials. *Applied Radiation and Isotopes, 54*(4), 687-689.

Beretka, J., & Mathew, P. (1985). Natural radioactivity of Australian building materials, industrial wastes and by-products. *Health physics, 48*(1), 87-95.

Desouky, O., Ding, N., & Zhou, G. (2015). Targeted and non-targeted effects of ionizing radiation. *Journal of Radiation Research and Applied Sciences, 8*(2), 247-254.

Dizman, S., Görür, F. K., Keser, R., & Görür, O. (2019). The assessment of radioactivity and radiological hazards in soils of Bolu province, Turkey. *Environmental Forensics, 20*(3), 211-218.

Dondi, M. (1999). Clay materials for ceramic tiles from the Sassuolo District (Northern Apennines, Italy). Geology, composition and technological properties. *Applied Clay Science, 15*(3-4), 337-366.

Engelkemeir, D., Flynn, K., & Glendenin, L. (1962). Positron emission in the decay of K 40. *Physical Review, 126*(5), 1818.

Ferrari, F., & Szuszkiewicz, E. (2022). Health hazards posed by ionizing radiation to human space missions and newly developing methodologies to investigate them. *bioRxiv*, 2022.2003. 2028.486099.

Gaffney, J. S., & Marley, N. A. (2006). Radionuclide sources *Radionuclide concentrations in food and the environment* (pp. 23-36): CRC Press.

Gilmore, G. (2008). *Practical gamma-ray spectroscopy*: John Wiley & Sons.

Graef, F., Schneider, I., Fasse, A., Germer, J., Gevorgyan, E., Haule, F., . . . Kissoly, L. (2015). Natural resource management and crop production strategies to improve regional food systems in Tanzania. *Outlook on Agriculture, 44*(2), 159-167.

Hameed, B. S., Kaddoori, F. F., & Fzaa, W. T. (2021). Concentrations and Radiation Hazard Indices of Naturally Radioactive Materials for Flour Samples in Baghdad Markets. *Baghdad Sci J, 18*(3), 0649.

ICRP. (1993). Protection against Rn-222 at home and at work. *International Commission on Radiological Protection Publication 65. Ann. ICRP, 23*(2).

ICRP. (2007). ICRP publication 103. *Ann ICRP, 37*(2.4), 2.

Janković, M. M., Rajačić, M., Rakić, T. M., & Todorović, D. (2013). Natural radioactivity in imported ceramic tiles used in Serbia. *Processing and Application of Ceramics, 7*(3), 123-127.

Joel, E., Maxwell, O., Adewoyin, O., Ehi-Eromosele, C., Embong, Z., & Oyawoye, F. (2018). Assessment of natural radioactivity in various commercial tiles used for building purposes in Nigeria. *MethodsX, 5*, 8-19.

Kebwaro, J. M., Rathore, I., Hashim, N., & Mustapha, A. (2011). Radiometric assessment of natural radioactivity levels around Mrima Hill, Kenya.

Kelleter, L., Radogna, R., Volz, L., Attree, D., Basharina-Freshville, A., Seco, J., . . . Jolly, S. (2020). A scintillator-based range telescope for particle therapy. *Physics in Medicine & Biology, 65*(16), 165001.

Kenyanya, O., Wachira, J. M., & Mbuvi, H. (2013). Determination of potassium levels in intensive subsistence agricultural soils in Nyamira County, Kenya.

Khan, K., Khan, H., Tufail, M., Khatibeh, A., & Ahmad, N. (1998). Radiometric analysis of Hazara phosphate rock and fertilizers in Pakistan. *Journal of environmental radioactivity, 38*(1), 77-84.

Kharisov, B. I., & Kharissova, O. V. (2013). 1 Main Ionizing Radiation Types and Their Interaction with Matter. *Radiation Synthesis of materials and Compounds*, 1-20.

Knapp. (2013). Targeted radionuclide therapy-an overview. *Current radiopharmaceuticals, 6*(3), 152-180.

Knipp, J., & Uhlenbeck, G. (1936). Emission of gamma radiation during the beta decay of nuclei. *Physica, 3*(6), 425-439.

Knoll, G. F. (2010). *Radiation detection and measurement*: John Wiley & Sons.

Krstić. (2007). Radioactivity of some domestic and imported building materials from South Eastern Europe. *Radiation measurements, 42*(10), 1731-1736.

Lee. (2005). Impact of entrepreneurship education: A comparative study of the US and Korea. *The international entrepreneurship and management journal, 1*, 27-43.

Mahur. (2008). Estimation of radon exhalation rate, natural radioactivity and radiation doses in fly ash samples from Durgapur thermal power plant, West Bengal, India. *Journal of environmental radioactivity, 99*(8), 1289-1293.

Matheson, F. (1966). Geology of the Kajiado area. *Geological Survey of Kenya Report, 70*.

Matsitsi. (2020). Radiometric survey of the Tyaa river sand mine in Kitui, Kenya. *Radiation protection dosimetry, 188*(4), 405-412.

McNaught, A. D., & Wilkinson, A. (1997). *Compendium of chemical terminology* (Vol. 1669): Blackwell Science Oxford.

Msanya, B. M., Magoggo, J. P., & Otsuka, H. (2002). Development of soil surveys in Tanzania. *Pedologist, 46*(2), 79-88.

Mustapha. (1999). Assessment of human exposures to natural sources of radiation in Kenya. *Radiation protection dosimetry, 82*(4), 285-292.

Nalianya, J. S., Waswa, M. N., Maingi, F., & Wanyama, C. K. (2022). Radiological measurement of hazardous levels in construction tiles in Bungoma county, Kenya. *ITEGAM-JETIA, 8*(33), 40-43.

Nataša, T., Jovana, N., Ivana, S., Hansman, J., Andrej, V., Predrag, K., . . . Sanja, B. (2020). Radioactivity in drinking water supplies in the Vojvodina region, Serbia, and health implication. *Environmental Earth Sciences, 79*(7).

Nyamai, C., Mathu, E., Wallbrecher, E., & Opiyo-Akech, N. (2001). A reappraisal of the geology, structures and tectonics of the Mozambique belt East of the Kenya Rift System.

Odumo, B. O. (2021). *Analysis and Multivariate Modeling of Heavy Metals and Associated Radiogenic Impact of Gold Mining in the Migori-Transmara Complex of Southwestern Kenya.* University of Nairobi.

World Health Organization. (2016). Global status report on blood safety and availability. *2016 Global status report on blood safety and availability.*

Otwoma, D., Patel, J., Bartilol, S., & Mustapha, A. (2012). Radioactivity and dose assessment of rock and soil samples from Homa Mountain, Homa Bay County, Kenya.

Otwoma, D., Patel, J., Bartilol, S., & Mustapha, A. (2013). Estimation of annual effective dose and radiation hazards due to natural radionuclides in mount Homa, southwestern Kenya. *Radiation protection dosimetry*, *155*(4), 497-504.

United Nations scientific Committee on the Effects of Atomic Radiation. (2017). *Sources, effects and risks of ionizing radiation,* (UNSCEAR) 2016 report: report to the general assembly, with scientific annexes: United Nations.

Ragheb, M. (2011). Gamma Rays Interaction with matter. *Nuclear, Plasma and Radiation Science. Inventing the Future," https://netfiles. uiuc. edu/mragheb/www*, 17-22.

Raghu, Y., Ravisankar, R., Chandrasekaran, A., Vijayagopal, P., & Venkatraman, B. (2017). Assessment of natural radioactivity and radiological hazards in building materials used in the Tiruvannamalai District, Tamilnadu, India, using a statistical approach. *Journal of Taibah University for Science*, *11*(4), 523-533.

Rami. (2007). Perception Digital Test (PDT) for the assessment of incipient visual disorder in initial Alzheimer's disease. *Neurologia (Barcelona, Spain)*, *22*(6), 342-347.

Ravisankar, R., Vanasundari, K., Chandrasekaran, A., Rajalakshmi, A., Suganya, M., Vijayagopal, P., & Meenakshisundaram, V. (2012). Measurement of natural radioactivity in building materials of Namakkal, Tamil Nadu, India using gamma-ray spectrometry. *Applied Radiation and Isotopes*, *70*(4), 699-704.

Richards, S. (1999). *Eighteenth-century ceramics: Products for a civilised society*: Manchester University Press.

Righi. (2009). Natural radioactivity in Italian ceramic tiles. *Radioprotection*, *44*(5), 413-419.

Righi, S., & Bruzzi, L. (2006). Natural radioactivity and radon exhalation in building materials used in Italian dwellings. *Journal of environmental radioactivity*, *88*(2), 158-170.

Saif Eldin, A., Radwan, N., & Khalifa, E. (2022). Evaluation of occupational indoor heat stress impact on health and kidney functions among kitchen workers. *Egyptian Journal of Occupational Medicine, 46*(3), 93-108.

Senthilkumar, G., Raghu, Y., Sivakumar, S., Chandrasekaran, A., Anand, D. P., & Ravisankar, R. (2014). Natural radioactivity measurement and evaluation of radiological hazards in some commercial flooring materials used in Thiruvannamalai, Tamilnadu, India. *Journal of Radiation Research and Applied Sciences, 7*(1), 116-122.

Senthilkumar, R., & Narayanaswamy, R. (2016). Assessment of radiological hazards in the industrial effluent disposed soil with statistical analyses. *Journal of Radiation Research and Applied Sciences, 9*(4), 449-456.

Siraz, M. M., Dewan, M. J., Chowdhury, M. I., Al Mahmud, J., Alam, M., Rashid, M. B., . . . Yeasmin, S. (2023). Radioactivity in soil and coal samples collected from the vicinity of the coal-fired thermal power plant and evaluation of the associated hazard parameters. *International Journal of Environmental Analytical Chemistry*, 1-18.

Steinhauser, G., & Buchtela, K. (2012). Handbook of radioactivity analysis. *Handb. Radioact. Anal, 3*.

Stoulos, S., Manolopoulou, M., & Papastefanou, C. (2003). Assessment of natural radiation exposure and radon exhalation from building materials in Greece. *Journal of environmental radioactivity, 69*(3), 225-240.

Tsai, T.-L., Lin, C.-C., Wang, T.-W., & Chu, T.-C. (2008). Radioactivity concentrations and dose assessment for soil samples around nuclear power plant IV in Taiwan. *Journal of radiological protection, 28*(3), 347.

UNSCEAR. (1988). Sources and Effects of Ionizing Radiation, United Nations Scientific Committee on the Effects of Atomic Radiation (UNSCEAR) 1988 Report, Volume I: Report to the General Assembly, with Scientific Annexes-Sources

UNSCEAR. (2000). Sources and Effects of Ionizing Radiation, United Nations Scientific Committee on the Effects of Atomic Radiation (UNSCEAR) 2000 Report, Volume I: Report to the General Assembly, with Scientific Annexes-Sources *New Yor*, 453-487.

UNSCEAR. (2010). Sources and Effects of Ionizing Radiation, United Nations Scientific Committee on the Effects of Atomic Radiation (UNSCEAR) 2010 Report, Volume I: Report to the General Assembly, with Scientific Annexes-Sources.

Uosif, M., Issa, S. A., & Abd El-Salam, L. (2015). Measurement of natural radioactivity in granites and its quartz-bearing gold at El-Fawakhir area (Central Eastern Desert), Egypt. *Journal of Radiation Research and Applied Sciences, 8*(3), 393-398.

Venugopal, V., & Bhagdikar, P. S. (2012). de Broglie Wavelength and Frequency of the Scattered Electrons in Compton Effect. *arXiv preprint arXiv:1202.4572*.

Wang, W. (2003). The operational characteristics of a sodium iodide scintillation counting system as a single-channel analyzer. *Radiation protection management, 20*(5), 28-36.

Xinwei, L. (2005). Natural radioactivity in some building materials of Xi'an, China. *Radiation measurements, 40*(1), 94-97.

APPENDICES

APPENDIX 1: Sample Tiles Collected Before Crushing.

APPENDIX 2: Labeling of the Tile Samples.

APPENDIX 3: The Crusher /Pulverizer Machine used at the Ministry of Mining and Petroleum Headquarters Nairobi-Kenya.

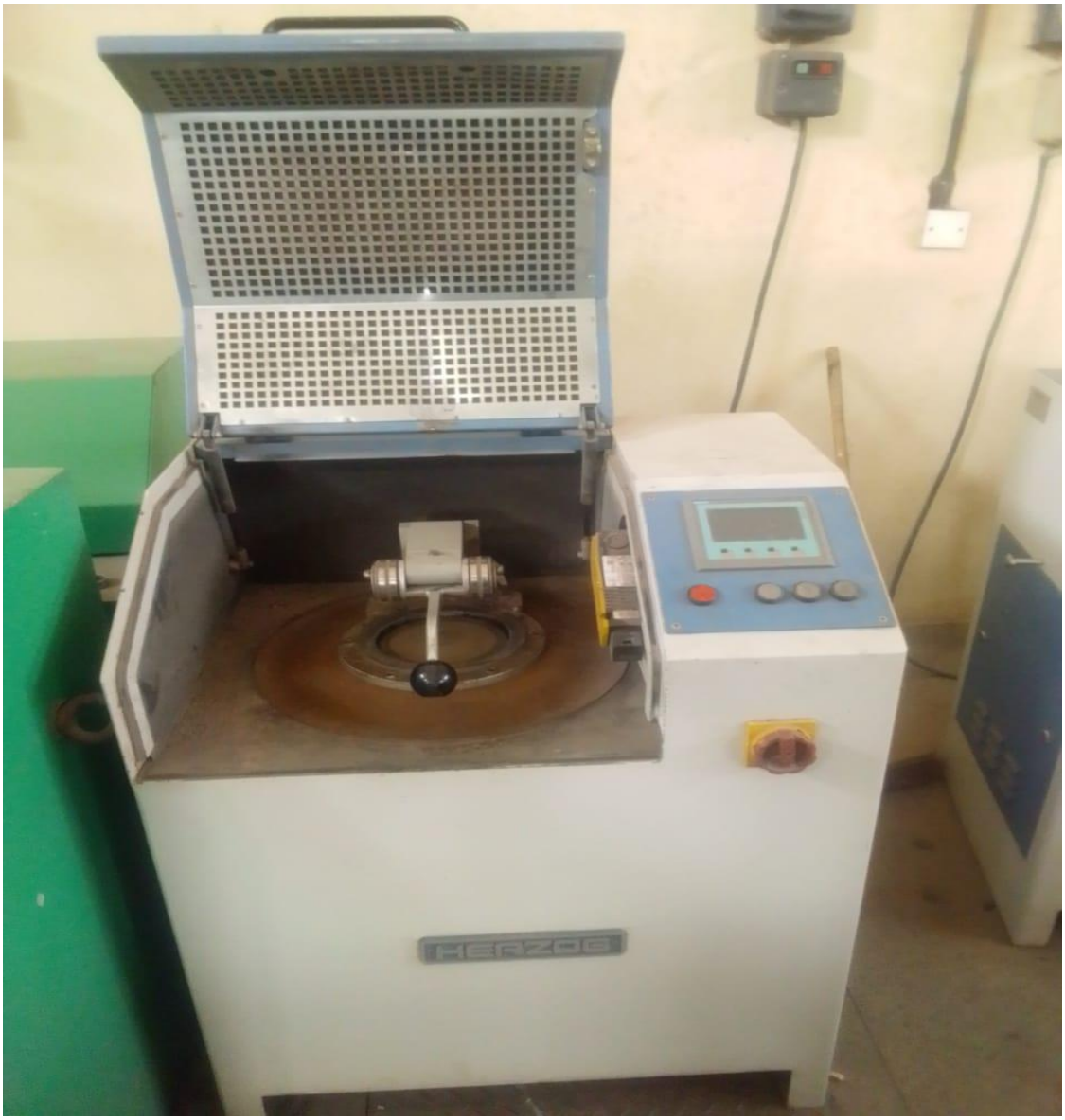

APPENDIX 4: Weighing the Tile Samples for Packaging at South Eastern Kenya University.

APPENDIX 5: Packaging of the Tile Samples at South Eastern Kenya University.

APPENDIX 6: Sodium Iodide Gamma Ray Spectrometer used in the Study (Outer View)